

The Economics of Digital Intelligence Capital: Endogenous Depreciation and the Structural Jevons Paradox

Yukun Zhang

The Chinese University Of Hongkong
HongKong, China
215010026@link.cuhk.edu.cn

Tianyang Zhang

University of Macau
Macau, China
yc57317@um.edu.mo

January 21, 2026

Abstract

This paper develops a micro-founded economic theory of the AI industry by modeling large language models as a distinct asset class—Digital Intelligence Capital—characterized by data–compute complementarities, increasing returns to scale, and relative (rather than absolute) valuation. We show that these features fundamentally reshape industry dynamics along three dimensions. First, because downstream demand depends on relative capability, innovation by one firm endogenously depreciates the economic value of rivals’ existing capital, generating a persistent innovation pressure we term the Red Queen Effect. Second, falling inference prices induce downstream firms to adopt more compute-intensive agent architectures, rendering aggregate demand for compute super-elastic and producing a structural Jevons paradox. Third, learning from user feedback creates a data flywheel that can destabilize symmetric competition: when data accumulation outpaces data decay, the market bifurcates endogenously toward a winner-takes-all equilibrium. We further characterize conditions under which expanding upstream capabilities erode downstream application value (the Wrapper Trap). A calibrated agent-based model confirms these mechanisms and their quantitative implications. Together, the results provide a unified framework linking intelligence production upstream with agentic demand downstream, offering new insights into competition, scalability, and regulation in the AI economy.

1 Introduction

The rapid diffusion of large language models (LLMs) has introduced a new class of productive assets into the global economy. Unlike earlier general-purpose technologies—such as electricity, information technology, or the internet—generative AI does not merely augment existing factors of production or reduce transaction costs. Instead, it produces a scalable stock of general cognitive capability that can perform reasoning, coding, planning, and decision-making tasks traditionally associated with skilled human labor. Investment in this capability has reached unprecedented levels: annual expenditures on AI training

and inference infrastructure now rival the GDP of mid-sized economies, while competitive advantage appears increasingly concentrated in a small number of firms.

Yet this rapid expansion is accompanied by a set of puzzling and seemingly contradictory economic patterns. Despite dramatic declines in the unit cost of intelligence (e.g., inference costs per token), aggregate compute demand continues to surge rather than stabilize. Downstream application developers face persistently low and fragile profit margins, even as upstream providers report high revenues. Most strikingly, market leadership in foundation models appears unusually unstable: firms that pause innovation experience rapid erosion of economic value, while small early advantages can escalate into winner-takes-all dominance. Standard economic frameworks struggle to jointly explain these phenomena.

Existing theories of technological change offer only partial guidance. In neoclassical and endogenous growth models, technology typically enters as an exogenous or semi-exogenous productivity shifter, leaving the competitive dynamics of technological capital largely unexplored. Task-based models of automation emphasize labor displacement and task reallocation but abstract from the industrial organization of AI supply. Meanwhile, the economics of software platforms focuses on near-zero marginal costs, overlooking the severe physical capacity constraints and rapid obsolescence characteristic of large-scale AI systems. As a result, the literature lacks a unified framework that links the production of intelligence upstream with the organization of agentic demand downstream.

This paper proposes such a framework. We introduce Digital Intelligence Capital as a distinct asset class and develop a dynamic, micro-founded model of the AI production stack. Digital Intelligence Capital differs fundamentally from traditional capital and knowledge in three respects. First, it is produced through a data–compute synthesis technology that exhibits strong complementarities and increasing returns to scale. Second, its economic value is relative rather than absolute: a model’s profitability depends on its capability advantage vis-à-vis competitors and the technological frontier. Third, it functions as a non-rival but capacity-constrained intermediate input into a downstream ecosystem of AI agents. These properties imply that depreciation, demand, and market structure are endogenously intertwined.

Our analysis yields three core theoretical results—which together characterize the structural dynamics of the AI economy.

First, we derive Endogenous Economic Depreciation. Because downstream demand is sensitive to relative capability, investment by one firm imposes a negative pecuniary externality on rivals by reducing the shadow value of their existing intelligence capital. We show that even a market leader experiences rapid economic depreciation if it fails to keep pace with frontier growth—a phenomenon we term the Red Queen Effect. In equilibrium, firms must continuously invest simply to maintain their relative position, generating a persistent “innovation tax” that is absent from standard capital accumulation models.

Second, we establish a Structural Jevons Paradox on the demand side. As the unit price of intelligence falls, downstream firms do not merely scale output along a fixed production function. Instead, they endogenously redesign their agent architectures—adopting deeper reasoning loops, larger memory contexts, and tool-augmented workflows—that dramatically increase compute intensity. We prove that under general conditions, this architectural response renders aggregate demand for compute super-elastic, so that efficiency gains raise total resource consumption and industry revenue.

Third, we characterize the Data Flywheel as a dynamic bifurcation mechanism. Superior models attract greater usage, which generates proprietary feedback data that further

enhances model quality. We show that when data learning efficiency exceeds a critical threshold relative to data depreciation, the symmetric oligopoly becomes dynamically unstable. The industry then bifurcates into a winner-takes-all equilibrium, even in the absence of predatory pricing or entry barriers. Market concentration thus emerges as a structural property of the production technology rather than a purely strategic outcome.

In addition, we analyze the vertical relationship between foundation models and downstream applications. As upstream general capabilities expand, they may substitute for—rather than complement—downstream orchestration capital. We formalize this mechanism as the Wrapper Trap, identifying conditions under which application-layer firms face systematic erosion of value as the frontier advances.

To quantify these mechanisms beyond local analytical results, we complement the theory with a calibrated agent-based model. The numerical analysis verifies the Red Queen depreciation channel, the super-elastic demand response underlying the Jevons paradox, the existence of a flywheel stability threshold, and the long-run viability conditions for the downstream ecosystem. Importantly, the simulations introduce no additional mechanisms beyond those derived analytically; they serve to expose the global dynamics implied by the theory.

The paper proceeds as follows. Section 2 describes the economic environment and industry structure. Section 3 defines Digital Intelligence Capital and its production technology. Section 4 characterizes the static upstream market equilibrium. Sections 5–8 derive the dynamic laws governing endogenous depreciation, architectural demand shifts, data-driven market concentration, and vertical cannibalization. Section 9 presents the numerical analysis. Section 10 discusses policy implications and concludes.

Figure 1 provides an overview of the economic environment and the feedback structure studied in this paper. It highlights the vertical organization of the AI industry and situates the three core mechanisms—endogenous depreciation (Red Queen effect), super-elastic demand (structural Jevons paradox), and data-driven market concentration—within a unified dynamic framework.

2 Literature

With breakthrough advancements in Artificial Intelligence (AI) technology, insights and perspectives regarding how AI shapes the economy have expanded significantly. The fundamental understanding of how AI reshapes the economy rests on how AI enters or influences the production function. The literature reveals that AI has evolved from a simple factor of “capital deepening” into a disruptive force that alters the structure of production functions (task-based models), lowers prediction costs (micro-foundations), and reshapes innovation processes (ideas production functions).

Early models attempted to incorporate AI into traditional capital terms (K) or total factor productivity terms (A). In the traditional Solow growth model, technological progress is typically treated as exogenous Total Factor Productivity (TFP) or simple labor-augmenting progress. However, with the rise of Artificial Intelligence (AI), economists discovered that traditional frameworks struggled to capture the specificity of AI—it functions simultaneously as capital (machinery) and labor (capable of executing cognitive tasks), while also possessing the capacity to alter innovation itself like a General Purpose Technology (GPT) defined by Bresnahan and Trajtenberg (1995). Referring to the basic framework for intangible asset accounting by Corrado et al. (2009), we have a theoretical starting point for understanding its AI model as an intermediate capital good.

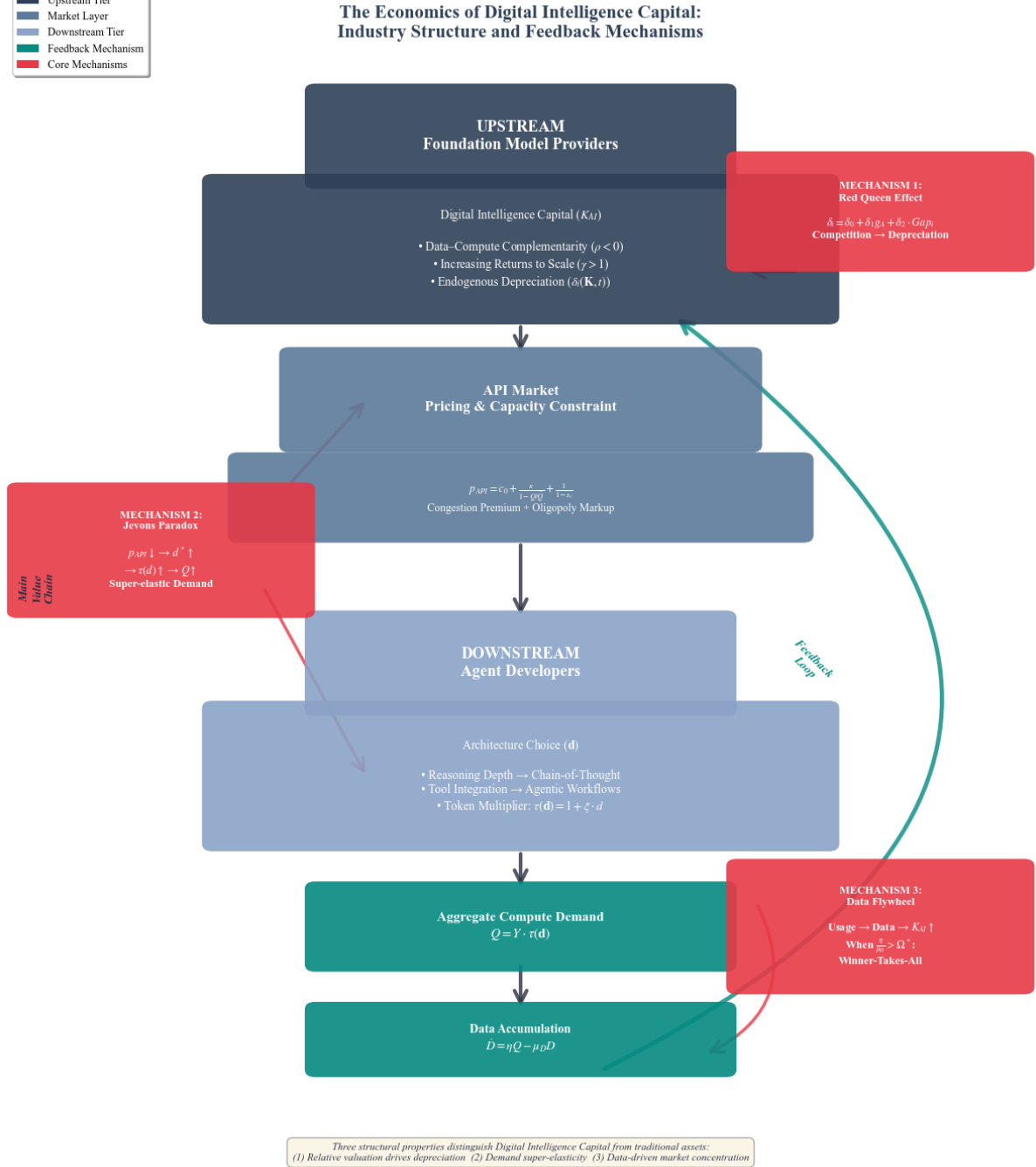
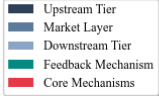


Figure 1: Industry structure and feedback mechanisms of digital intelligence capital. The figure illustrates the vertical structure of the AI production stack and the three core mechanisms analyzed in the paper. *Upstream*, foundation model providers invest in digital intelligence capital K_{AI} , characterized by data-compute complementarity, increasing returns to scale, and endogenous economic depreciation. AI services are intermediated through an API market with capacity constraints and oligopolistic markups. *Downstream*, agent developers optimally choose architecture complexity (e.g., reasoning depth, tool integration), which amplifies token usage via a token multiplier. Falling API prices induce more compute-intensive architectures, generating super-elastic demand (Jevons paradox). Aggregate usage produces proprietary feedback data, which feeds back into upstream capability accumulation. When data accumulation dominates data decay, the feedback loop destabilizes symmetric competition and leads to winner-takes-all outcomes.

Currently, the dominant framework for analyzing the impact of AI on employment and productivity is the task-based model proposed by Zeira (1998), Autor et al. (2003) and refined by Acemoglu and Restrepo (2018). This theory does not view production simply as a combination of capital and labor, but rather as a collection of tasks. Task models reveal automation's three effects—displacement, productivity gains, and reinstatement—where new task creation determines long-run labor share (Acemoglu and Restrepo, 2018, 2019, 2022). However, caution must also be exercised regarding the trap of “so-so automation” resulting from excessive automation. Recent empirical studies have provided granular evidence on AI's heterogeneous impact (Brynjolfsson et al., 2023; Noy and Zhang, 2023). This suggests that AI might not only displace tasks but also reshape the wage structure by altering the relative scarcity of cognitive skills (Autor, 2024).

Another line of inquiry focuses on how AI enters the “ideas production function,” influencing long-term economic growth rates. AI enters the “ideas production function” by automating R&D, potentially transforming linear growth into super-exponential trajectories (Aghion et al., 2017; Acemoglu and Johnson, 2024; Korinek, 2023; Jones, 2022).

Many scholars also focus on the specific functions of AI within micro-production processes. Agrawal et al. (2018) propose that the essence of AI in the production function is a “precipitous drop in prediction costs.” Furthermore, Agrawal et al. (2022) distinguish between “point solutions” and “system-level solutions,” noting that a qualitative leap in the production function occurs only when production processes are reorganized around the predictive capabilities of AI. The emphasis on system-level reorganization mirrors the seminal argument by Brynjolfsson and Hitt (2000). The historical observation by Alcott (2005) that improved energy efficiency can actually lead to increased total resource consumption also provides a perspective for research in the digital economy. Drawing on Saunders (1992)'s theoretical argument on the elasticity of substitution within a neoclassical growth framework, the introduction of the "Structural Jevons Paradox" further expands this perspective.

Research on AI and the economy, particularly production, cannot avoid examining AI itself. Regarding AI development, computing power infrastructure represents the most critical bottleneck; the global AI server market is projected to reach 400 billion USD by 2025, with China accounting for a 40% share yet remaining dependent on imported foundational chips (Stanford HAI, 2025). High-quality data is proving superior to model size alone; small models trained on refined data are achieving performance comparable to large models, indicating diminishing marginal returns to scale laws (Microsoft Research, 2025). Data depletion pushes AI toward a “data-constrained” regime. Villalobos et al. (2024) predict high-quality language data exhaustion by 2028, requiring synthetic data and recursive training (Kaplan et al., 2020). This necessitates endogenizing data as finite reproducible resource, distinct from physical capital (Jones, 2022; Korinek, 2023).

However, a critical theoretical gap remains. Existing literature largely bifurcates into two extremes: macro-level growth models that treat AI as a generic TFP shock (A), and micro-level task models that focus on labor substitution at the specific job level. **What is missing is a structural equilibrium model that connects the "production of intelligence" upstream with the "application of agents" downstream.**

Current frameworks often overlook the unique industrial organization of the AI sector—specifically, its Two-tier Production Structure. Foundation models are not final consumption goods but intermediate "Digital Intelligence Capital" subject to rapid endogenous depreciation and massive scale effects. The interaction between upstream capacity constraints (supply) and downstream architectural choices (demand) creates complex

pricing and innovation dynamics that standard models fail to capture.

Therefore, this chapter seeks to bridge this gap. By endogenizing the production of foundation models and the architectural decisions of agents within a unified vertical framework, we provide a new theoretical lens to explore the **Artificial Intelligence Production Function**, explaining phenomena from the "Red Queen" innovation race to the "Jevons Paradox" in compute consumption.

3 Economic Environment and Industry Structure

We consider a continuous-time economy indexed by $t \in [0, \infty)$. The economy is characterized by a vertical industrial organization comprising two distinct tiers of production: an upstream oligopoly of foundation model providers and a downstream continuum of specialized agent developers. The market is populated by a representative household that consumes the final services produced by the downstream sector.

To focus on the supply-side dynamics of the artificial intelligence industry, we assume a small open economy setting where the risk-free interest rate $r > 0$ is exogenously given. All firms maximize the net present value (NPV) of their profit flows discounted at rate r .

3.1 The Upstream Tier: Foundation Model Providers

The upstream sector consists of a finite set of firms, denoted by $\mathcal{N} = \{1, 2, \dots, N\}$, where N is a small integer reflecting the oligopolistic nature of the industry driven by high entry barriers. Each upstream firm $i \in \mathcal{N}$ engages in the production of a unique asset class, denoted by the stock variable $K_{AI,i}(t) \in \mathbb{R}_+$.

Unlike traditional physical capital, $K_{AI,i}$ represents the general cognitive capability of the foundation model, such as reasoning, coding, and language understanding. It functions as an intermediate capital good that is non-rival but partially excludable. Firm i monetizes this capital by selling inference services—quantified as API tokens $Q_i(t)$ —to downstream agents. Consequently, upstream firms compete strategically in both prices and R&D investment to maximize intertemporal profits, subject to the capacity constraints of their physical compute clusters.

3.2 The Downstream Tier: Agent Developers

The downstream sector consists of a continuum of application developers, indexed by $j \in [0, M_t]$, where the measure of active firms M_t is endogenously determined by a free-entry condition. Each downstream firm j produces a differentiated service variety $Y_j(t)$ by combining upstream intelligence with firm-specific inputs.

Crucially, firm j possesses a specialized stock of intangible capital $O_j(t)$, which we term *Orchestration Capital*. This asset encapsulates the firm's proprietary middleware, prompt engineering libraries, and domain-specific context that allow it to effectively wield the general-purpose foundation model. These firms operate under monopolistic competition; each faces a downward-sloping demand curve for its specific variety Y_j , allowing it to set prices above marginal cost to cover fixed development costs.

3.3 The Technological Frontier

The production of digital intelligence is constrained by the global state of technology. We explicitly distinguish between the exogenous global frontier and firm-specific productivity.

Assumption 3.1 (Technological Frontier). *Let $\bar{A}(t)$ denote the Global Technological Frontier, representing the theoretical maximum efficiency of current algorithmic architectures (e.g., Transformer efficiency) and hardware capabilities. We assume $\bar{A}(t)$ evolves exogenously according to:*

$$\frac{\dot{\bar{A}}(t)}{\bar{A}(t)} = g_A, \quad \bar{A}(0) = A_0 \quad (1)$$

where $g_A > 0$ is the constant rate of exogenous technical progress.

While the frontier $\bar{A}(t)$ is public information, the effective Total Factor Productivity (TFP) of a specific upstream firm i , denoted by $A_i(t)$, depends on its private accumulation of basic research R_i . Specifically, we posit $A_i(t) = \bar{A}(t) \cdot \xi(R_i)$, where $\xi(\cdot)$ is an increasing, concave function reflecting the firm's absorptive capacity.

3.4 Information Structure and Timing

We assume perfect information regarding the current state vectors $\mathbf{K}(t)$ and $\mathbf{O}(t)$, as well as rational expectations regarding the evolution of the technological frontier $\bar{A}(t)$ and the strategic actions of competitors.

Although the model is set in continuous time, the logical sequence of events at each instant t proceeds as follows: first, upstream and downstream firms make simultaneous innovation decisions to accumulate $K_{AI,i}$ and O_j ; second, upstream firms set API prices $p_{API,i}$ subject to capacity constraints; third, downstream firms observe prices and qualities to determine their optimal architecture and clear the market; finally, capital stocks depreciate according to the endogenous mechanisms defined in Sections 4 and 8.

4 Digital Intelligence Capital

Central to our framework is the conceptualization of foundation models not merely as software or technology, but as a distinct asset class: **Digital Intelligence Capital**. In this section, we formally define this asset and characterize its unique production technology and depreciation properties, which distinguish it from traditional physical capital (K) and human capital (L).

4.1 Definition and Economic Attributes

Definition 4.1 (Digital Intelligence Capital). *Let $K_{AI,i}(t) \in \mathbb{R}_+$ denote the stock of general-purpose cognitive capability possessed by firm i at time t . It acts as an intermediate input in the production of downstream services, characterized by three distinct economic attributes.*

First, the asset is non-rival. The stock $K_{AI,i}$ is not depleted by usage; once trained, the model can serve an infinite stream of inference requests, subject only to physical compute throughput constraints. Second, it exhibits partial excludability. Unlike pure public knowledge, $K_{AI,i}$ is excludable via API access controls, yet it faces leakage risks (e.g., via distillation or weight theft) that differentiate it from strictly proprietary physical assets.

Finally, its formation requires cumulative synthesis, representing the irreversible compression of information from vast datasets into synaptic weights through massive upfront investment.

4.2 Property 1: The Intelligence Production Function

How is Digital Intelligence Capital created? We model the accumulation process using a micro-founded Augmented CES technology. Unlike standard industrial production, the generation of intelligence is constrained by the information-theoretic limits of learning from data.

The law of motion for capital accumulation is given by:

$$\dot{K}_{AI,i}(t) = \mathcal{F}(C_i, D_{eff,i}) - \delta_i(t)K_{AI,i}(t) \quad (2)$$

We specify the gross production function $\mathcal{F}(\cdot)$ as:

$$\mathcal{F}(C_i, D_{eff,i}) = \underbrace{A_i(t)}_{\text{Firm TFP}} \cdot \underbrace{[\alpha C_i(t)^\varrho + (1 - \alpha)D_{eff,i}(t)^\varrho]^\frac{\gamma}{\varrho}}_{\text{Compute-Data Synthesis}} \quad (3)$$

where C_i represents compute flow (FLOPs) and $D_{eff,i}$ represents the effective data stock. The parameters ϱ and γ are calibrated to empirical scaling laws.

Microfoundation of Complementarity ($\varrho < 0$). The choice of the substitution parameter ϱ is derived from the empirical structure of Neural Scaling Laws. [?](#) establish that the prediction loss L scales as a function of compute and data, $L(C, D) = E + AC^{-\phi} + BD^{-\phi}$. This functional form implies that compute (C) and data (D) operate under strict *structural complementarity*.

Specifically, if one were to increase compute $C \rightarrow \infty$ while holding data D fixed, the loss would converge to a non-zero floor determined by irreducible entropy (the "data bottleneck"). No amount of additional compute can extract information that does not exist in the dataset. Economically, this behavior is isomorphic to a CES production function with a low elasticity of substitution, $\sigma = \frac{1}{1-\varrho} < 1$. Accordingly, we set $\varrho = -0.2$ ($\sigma \approx 0.83$), treating inputs as gross complements.

Microfoundation of Increasing Returns ($\gamma > 1$). The parameter γ characterizes returns to scale. A seeming contradiction arises here: engineering metrics (such as Cross-Entropy Loss) typically show diminishing returns to scale, yet the economic utility of these models exhibits increasing returns. We resolve this by distinguishing between *technical performance* and *economic utility*.

While technical scaling is concave—reducing the next-token prediction loss becomes exponentially harder as the model scales—the mapping to economic utility is convex. As formalized by the literature on "emergent capabilities" [\(?\)](#), task performance often follows a sigmoid or exponential relationship with loss reduction. The aggregate production function captures this composite effect. We calibrate $\gamma = 1.3$, reflecting that in the current technological regime, the marginal economic value of intelligence accelerates as models cross critical capability thresholds (e.g., gaining the ability to reason or code).

4.3 Property 2: Relative Value and Endogenous Obsolescence

The third and most critical property of Digital Intelligence Capital is that its economic value is determined *relatively*, rather than absolutely.

Assumption 4.1 (Relative Value Hypothesis). *The shadow price $q_i(t)$ of the capital stock $K_{AI,i}$ depends negatively on the aggregate state of the industry \mathbf{K}_{-i} :*

$$\frac{\partial q_i}{\partial K_{AI,j}} < 0, \quad \forall j \neq i \quad (4)$$

Intuitively, in a standard Solow growth model, a machine's productive capacity is independent of a competitor's investment. In the AI market, however, the value of model i is defined by its *comparative advantage* over model j . If the global technological frontier moves forward ($\bar{A} \uparrow$) or a competitor innovates ($K_{AI,j} \uparrow$), the effective demand for model i collapses. This renders $K_{AI,i}$ economically obsolete even if its physical weights remain unchanged. This property serves as the basis for the derivation of the endogenous economic depreciation function $\delta_i(t)$ presented in Section 4.

5 Upstream Market Equilibrium: The Static Core

In this section, we construct the static equilibrium of the foundation model market. We depart from standard Bertrand competition models by introducing two critical features specific to the AI industry: vertical differentiation based on digital intelligence capital, modeled via a Logit demand system, and strict physical capacity constraints on inference compute, which sustain markups even under intense price competition.

5.1 Downstream Demand for Foundation Models

Consider the decision problem of the continuum of downstream agents $j \in [0, M_t]$. At each instant t , agent j selects a single foundation model supplier $i \in \mathcal{N}$ to maximize its operational utility. We specify the indirect utility function V_{ji} as:

$$V_{ji}(t) = \theta \ln K_{AI,i}(t) - p_{API,i}(t) + \varepsilon_{ji}(t) \quad (5)$$

where $p_{API,i}$ is the price per token and ε_{ji} represents an idiosyncratic preference shock, assumed to follow an i.i.d. Type I Extreme Value distribution. The parameter $\theta > 0$ governs the elasticity of substitution with respect to model intelligence; a higher θ implies that downstream agents are highly sensitive to capability differences, favoring "smarter" models.

Aggregating over the continuum of agents, the market share $s_i(t)$ of firm i takes the standard multinomial Logit form:

$$s_i(\mathbf{p}, \mathbf{K}) = \frac{K_{AI,i}(t)^\theta \exp(-p_{API,i}(t))}{\sum_{k=1}^N K_{AI,k}(t)^\theta \exp(-p_{API,k}(t))} \quad (6)$$

Let $Q_{total}(t)$ denote the aggregate token demand of the economy. The specific demand faced by firm i is thus $Q_i(t) = s_i(\mathbf{p}, \mathbf{K}) \cdot Q_{total}(t)$. This demand structure captures the notion of *vertical differentiation*: firms with higher Digital Intelligence Capital $K_{AI,i}$ command larger market shares, ceteris paribus, but do not capture the entire market due to heterogeneous user preferences.

5.2 Capacity Constraints and the Cost Structure

A central economic feature of the AI industry is the rigidity of physical compute clusters. Unlike traditional software where marginal costs are near zero and capacity is elastic, AI inference is bounded by the physical throughput of GPUs (\bar{Q}). As demand approaches this limit, latency increases and system stability degrades. To capture this, we model the operational cost $C_{ops}(Q_i)$ using a convex barrier function:

$$C_{ops}(Q_i) = c_0 Q_i - \kappa \bar{Q} \ln \left(1 - \frac{Q_i}{\bar{Q}} \right) \quad (7)$$

where c_0 represents the constant baseline marginal cost (e.g., electricity), and $\kappa > 0$ scales the congestion penalty.

The convexity of this function plays a crucial role in market equilibration. As $Q_i \rightarrow \bar{Q}$, the marginal cost of serving an additional token approaches infinity. This structural constraint prevents the "Bertrand Paradox"—where prices collapse to marginal cost—by forcing firms to internalize the congestion externalities of aggressive pricing.

5.3 Optimal Pricing and the Congestion Markup

Each upstream firm i chooses its price $p_{API,i}$ to maximize instantaneous profit $\pi_i = p_{API,i} Q_i - C_{ops}(Q_i)$, taking competitors' prices as given. The first-order condition for profit maximization equates marginal revenue to marginal cost. Rearranging terms reveals the optimal pricing rule:

$$p_{API,i}^* = \underbrace{c_0}_{\text{Base Cost}} + \underbrace{\frac{\kappa}{1 - Q_i^*/\bar{Q}}}_{\text{Congestion Premium}} + \underbrace{\frac{1}{1 - s_i^*}}_{\text{Oligopoly Markup}} \quad (8)$$

This pricing equation decomposes the equilibrium price into three distinct economic components. The first is the physical cost of electricity. The second is the *Congestion Premium*, which acts as a shadow price for capacity; as demand Q_i^* approaches the physical limit \bar{Q} , this term explodes, effectively rationing demand through price. The third term is the *Oligopoly Markup*, derived from the own-price elasticity of demand in the Logit model ($\eta_{ii} = -(1 - s_i)$). It reflects the firm's market power: firms with higher market share s_i face more inelastic demand and thus charge a higher markup.

5.4 Static Equilibrium Definition

We formalized the interaction described above as a static non-cooperative game.

Definition 5.1 (Static API Market Equilibrium). *Given the vector of Digital Intelligence Capital states $\mathbf{K}(t)$, a Static Equilibrium is defined as a pair of price and quantity vectors $(\mathbf{p}^*, \mathbf{Q}^*)$ such that the following conditions hold simultaneously:*

1. **Profit Maximization:** For every firm i , the price $p_{API,i}^*$ maximizes π_i given competitors' prices \mathbf{p}_{-i}^* .
2. **Market Clearing:** The quantity demanded matches the quantity supplied: $Q_i^* = s_i(\mathbf{p}^*, \mathbf{K}) Q_{total}$.

3. **Feasibility:** The equilibrium quantities satisfy the physical capacity constraints: $Q_i^* < \bar{Q}$ for all $i \in \mathcal{N}$.

For analytical tractability in the subsequent dynamic analysis, we will frequently refer to the *Symmetric Equilibrium*, where all firms possess identical capital stocks K_{AI} , charge equal prices p^* , and serve equal market shares $s^* = 1/N$.

6 Dynamics I: Endogenous Depreciation and the Red Queen Effect

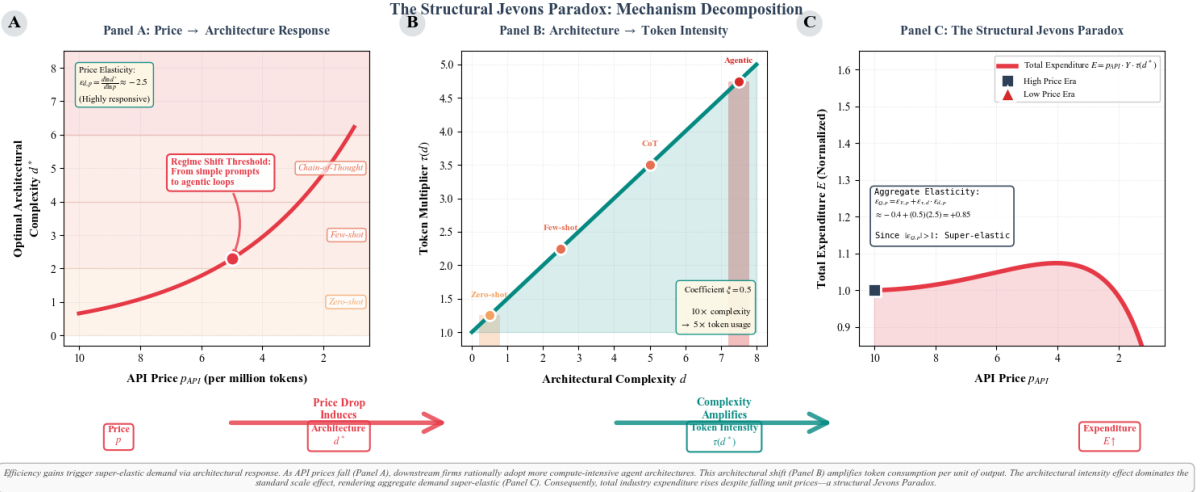


Figure 2: **The structural Jevons paradox: mechanism decomposition.** Panel A shows the downstream architectural response to declining API prices: as inference prices fall, firms optimally increase architectural complexity (e.g., reasoning depth and agentic loops), with a regime shift from simple prompting to agentic workflows. Panel B maps architectural complexity to token intensity, illustrating how more complex architectures amplify token usage through a token multiplier. Panel C combines these effects to show the resulting aggregate outcome: despite declining unit prices, total expenditure on AI services increases because the architecture-induced increase in token intensity dominates the standard scale effect. Together, the three panels demonstrate that the Jevons paradox in the AI industry is structural, arising from endogenous architectural choice rather than exogenous demand elasticity.

This section bridges the gap between static profit maximization and dynamic capital accumulation. We derive the core theoretical contribution of the paper: Endogenous Economic Depreciation. We demonstrate that in the AI industry, asset depreciation is not primarily a physical property of hardware or software decay, but a strategic outcome driven by the relative advancement of the technological frontier and the innovation of competitors.

6.1 The Shadow Value of Digital Intelligence Capital

We formulate the upstream firm's dynamic optimization problem using the Hamilton-Jacobi-Bellman (HJB) framework. Firm i chooses its investment flow $I_{AI,i}(t)$ to maximize

the present value of future profit streams, subject to the capital accumulation constraint. The value function $V_i(\mathbf{K}, t)$ satisfies the continuous-time Bellman equation:

$$rV_i(\mathbf{K}, t) = \max_{I_{AI,i}} \left\{ \pi_i^*(\mathbf{K}) - C_{RD}(I_{AI,i}) + \sum_{j=1}^N \frac{\partial V_i}{\partial K_{AI,j}} \dot{K}_{AI,j} + \frac{\partial V_i}{\partial t} \right\} \quad (9)$$

where $\pi_i^*(\mathbf{K})$ represents the reduced-form profit function derived from the static equilibrium in Section 3, and $C_{RD}(\cdot)$ is the convex cost of R&D investment.

Central to our analysis is the *shadow price* of digital intelligence capital, denoted by q_i . It represents the marginal increase in the firm's value resulting from an infinitesimal increase in its intelligence stock:

$$q_i(\mathbf{K}, t) \equiv \frac{\partial V_i}{\partial K_{AI,i}} \quad (10)$$

By applying the Envelope Theorem to the static profit function, we observe that the shadow price is proportional to the marginal revenue product of capital. Given the Logit demand structure, this yields $q_i \propto \theta \cdot s_i(1 - s_i)/K_{AI,i}$.

6.2 Mechanism: Pecuniary Externalities

The driver of endogenous depreciation is the sensitivity of firm i 's shadow price to the innovation of its rivals. In standard growth models, capital accumulation by one firm does not directly devalue the capital stock of another. In the AI market, however, vertical differentiation creates strong negative externalities.

Proposition 6.1 (Negative Pecuniary Externality). *An increase in the digital intelligence capital of a competitor j ($j \neq i$) strictly reduces the shadow value of firm i 's capital stock:*

$$\frac{\partial q_i}{\partial K_{AI,j}} < 0 \quad (11)$$

Proof Sketch. The market share s_i is determined by the ratio of firm i 's capability to the aggregate industry capability. An increase in $K_{AI,j}$ raises the denominator of the Logit function, strictly decreasing s_i . Since the marginal revenue product of capital is increasing in market share (for $s_i < 0.5$), the reduction in s_i lowers the marginal contribution of $K_{AI,i}$ to total profit. Consequently, the shadow price q_i falls. This cross-derivative mathematically captures the notion that "my model becomes worthless simply because your model became smarter." \square

6.3 Derivation of the Linearized Depreciation Function

We define the economic depreciation rate, $\delta_{econ,i}(t)$, as the negative rate of change of the shadow price relative to itself: $\delta_{econ,i} \equiv -\dot{q}_i/q_i$. Expanding the total time derivative of q_i reveals that depreciation is composed of self-cannibalization effects and competitive erosion.

To obtain a tractable functional form for the macroscopic model, we perform a Taylor expansion of $\delta_{econ,i}$ around the Symmetric Balanced Growth Path (BGP), where all firms grow at the rate of the exogenous frontier g_A . Let $Gap_i(t) \approx \ln(K_{-i}^{max}/K_{AI,i})$ denote the relative capability gap between firm i and the market leader.

$$\delta_i(t) = \delta_0 + \delta_1 g_A + \delta_2 \cdot \max\{0, \text{Gap}_i(t)\} \quad (12)$$

This linearized depreciation function, which we employ throughout the remainder of the paper, consists of three structural components:

- **Baseline Physical Depreciation (δ_0):** This term captures the standard wear and tear of physical servers and the maintenance cost of the codebase.
- **Frontier Pressure ($\delta_1 g_A$):** This term represents the "treadmill effect." We derive analytically that $\delta_1 = 1 + \theta(1 - \frac{1}{N})$. It implies that higher intelligence elasticity (θ) or a larger number of competitors (N) accelerates the obsolescence of existing models solely due to the movement of the global frontier $\bar{A}(t)$.
- **Competitive Gap Penalty ($\delta_2 \cdot \text{Gap}_i$):** This term captures the "Winner-Takes-All" dynamic. The parameter δ_2 , derived from the Hessian of the value function, dictates how strictly the market punishes laggards. A positive gap triggers accelerated depreciation, potentially driving the value of inferior models to zero.

6.4 Theorem 1: The Red Queen Effect

The existence of the frontier pressure term $\delta_1 g_A$ leads to a profound implication for firm strategy, which we term the Red Queen Effect.

Theorem 6.1 (The Red Queen Effect). *Consider a market leader with no competitive gap ($\text{Gap}_i = 0$). If this firm ceases innovation ($I_{AI,i} = 0$), the economic value of its digital intelligence capital does not remain constant but decays at the rate $\delta_0 + \delta_1 g_A$. To maintain a constant relative asset value, the firm must sustain a minimum investment intensity bounded by:*

$$\frac{I_{AI,i}}{\text{Rev}_i} \geq \frac{\delta_0 + \delta_1 g_A}{\mathcal{M}_{R&D}} \quad (13)$$

where $\mathcal{M}_{R&D}$ is the marginal productivity of R&D spending.

Proof. Suppose $I_{AI,i} = 0$. While the physical stock $K_{AI,i}$ remains constant (ignoring δ_0), the global frontier $\bar{A}(t)$ continues to advance at rate g_A . Consequently, the relative capability of the firm, defined as $\hat{k}_i = K_{AI,i}/\bar{A}(t)$, decays at rate g_A . Since the equilibrium price and market share depend on relative capability \hat{k}_i , the shadow price q_i collapses. The condition for $q_i = 0$ requires the firm to grow $K_{AI,i}$ at the same rate as the frontier g_A , necessitating the strictly positive investment flow defined above. \square

This theorem formalizes the "Innovation Tax" observed in the AI industry. Unlike traditional monopolies that can exploit a static moat, AI leaders are forced into aggressive capital expenditure cycles merely to preserve their current market standing. As the Red Queen in Lewis Carroll's *Through the Looking-Glass* remarks: "Now, here, you see, it takes all the running you can do, to keep in the same place."

7 Downstream Agents and Architecture Choice

In this section, we endogenize the technological adoption decision of downstream firms. Unlike previous literature that models AI adoption merely as a binary choice or a simple

Endogenous Economic Depreciation: The Relative Valuation of Digital Intelligence Capital

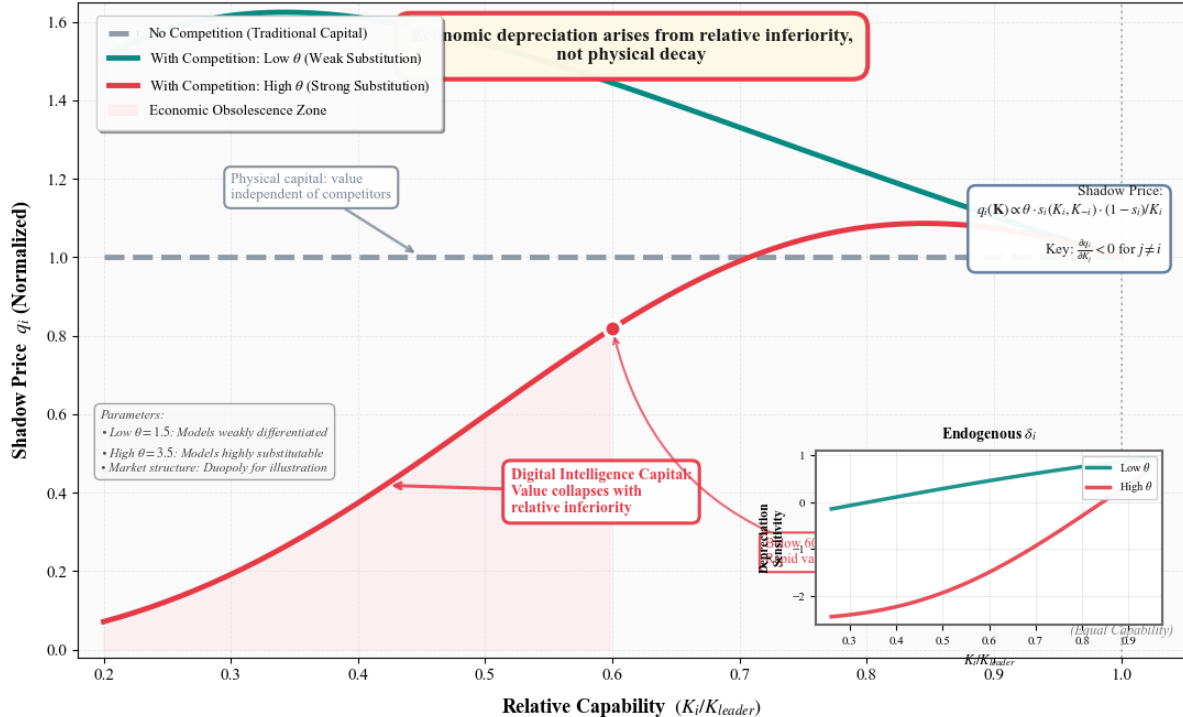


Figure 3: **Endogenous economic depreciation and the relative valuation of digital intelligence capital.** The figure illustrates how the shadow value of digital intelligence capital q_i depends on a firm's capability relative to the market leader. In the absence of competition, the value of capital remains constant, as in traditional physical capital. With competition, however, valuation becomes inherently relative: when models are weakly substitutable (low θ), the shadow price declines gradually with relative inferiority, whereas under strong substitutability (high θ), small capability gaps lead to sharp value collapse. The shaded region highlights an economic obsolescence zone in which capital loses value despite unchanged physical capacity. The inset panel shows the implied endogenous depreciation rate δ_i , which increases as relative capability deteriorates, capturing the Red Queen effect driven by competitive pressure rather than physical decay.

capital substitution, we posit that agent developers face a complex engineering trade-off: they must choose the optimal *architectural complexity* of their AI agents. This choice balances the marginal productivity of advanced reasoning capabilities against the marginal cost of increased token consumption.

7.1 The Agent Production Function

Firm j produces a specialized service Y_j . We model the production technology using a Cobb-Douglas form with constant returns to scale, augmented by an architectural efficiency term. The output is generated by combining labor L_j , the firm's specific orchestration capital O_j , and the effective intelligence derived from the upstream foundation model.

Specifically, the production function is given by:

$$Y_j = O_j \cdot [K_{AI}^{base} \cdot h(\mathbf{d}_j)]^{\psi_K} \cdot L_j^{1-\psi_K} \quad (14)$$

where $\psi_K \in (0, 1)$ represents the output elasticity of AI capital (calibrated to $\psi_K = 0.4$ in our numerical analysis), and K_{AI}^{base} is the raw capability of the chosen upstream model.

The term $h(\mathbf{d}_j)$ represents the *Architectural Efficiency Function*. It maps the design complexity vector \mathbf{d}_j —comprising reasoning depth (e.g., Chain-of-Thought steps), tool integration, and memory context—into a scalar productivity multiplier. We assume $h(\cdot)$ exhibits diminishing marginal returns with respect to complexity. For analytical tractability, we specify a scalar proxy for complexity $d_j \geq 0$:

$$h(d_j) = 1 + \phi \cdot d_j^\nu, \quad \nu \in (0, 1) \quad (15)$$

where $\phi > 0$ captures the efficacy of architectural engineering. This specification implies that "raw" intelligence ($d_j = 0$) yields a baseline efficiency of 1, while engineering efforts amplify the model's effective capability.

7.2 The Token Multiplier and Cost Structure

A critical feature of AI engineering is that complexity is not free. Advanced architectures such as recursive reasoning loops or massive context retrieval significantly increase the number of tokens required to produce a single unit of final service. We model this cost via the *Token Multiplier* function, $\tau(d_j)$.

The total API token demand $Q_{API,j}$ for firm j is the product of its service output and the token intensity of its architecture:

$$Q_{API,j} = Y_j \cdot \tau(d_j) \quad (16)$$

We assume the token cost rises linearly with complexity:

$$\tau(d_j) = 1 + \xi \cdot d_j \quad (17)$$

where $\xi > 0$ is the token consumption coefficient. This linear specification captures the reality that techniques like "Few-Shot Prompting" or "ReAct" linearly expand the context length per inference call.

7.3 Optimization and First-Order Conditions

Firm j acts as a price taker in the factor markets. It chooses the labor input L_j and the architectural complexity d_j to maximize profits. The profit maximization problem is:

$$\max_{L_j, d_j} \Pi_j = P_Y Y_j - wL_j - p_{API} Q_{API,j} \quad (18)$$

Substituting the constraints, the objective function becomes:

$$\max_{L_j, d_j} \{P_Y Y_j(L_j, d_j) - wL_j - p_{API} \tau(d_j) Y_j(L_j, d_j)\} \quad (19)$$

Note that the API cost is effectively a variable tax on production, where the tax rate $p_{API} \tau(d_j)$ is endogenously determined by the firm's engineering choices.

The first-order condition with respect to labor L_j yields the standard equality between the marginal revenue product and the wage. More importantly, the first-order condition with respect to architectural complexity d_j characterizes the optimal design choice:

$$\underbrace{(P_Y - p_{API} \tau) \frac{\partial Y_j}{\partial h} h'(d_j)}_{\text{Marginal Benefit of Intelligence}} = \underbrace{p_{API} \tau'(d_j) Y_j}_{\text{Marginal Cost of Tokens}} \quad (20)$$

Rearranging terms and using the specific functional forms, we derive the implicit solution for the optimal complexity d^* :

$$\frac{h'(d^*)}{h(d^*)} \cdot \frac{\psi_K}{\tau'(d^*)/\tau(d^*) + \Lambda} = \frac{p_{API} \tau(d^*)}{P_Y} \quad (21)$$

where Λ is a composite term of output elasticities.

This equilibrium condition reveals the central trade-off: firms increase architectural complexity until the elasticity of capability gain ($\frac{h'}{h}$) equals the shadow cost of token inflation. Crucially, Equation (21) shows that the optimal architecture d^* is a function of the API price p_{API} . As we will demonstrate in the subsequent section, this dependency is the structural driver of the Jevons Paradox.

8 Dynamics II: The Jevons Paradox as a Structural Result

In classical resource economics, the Jevons Paradox observes that technological improvements increasing the efficiency of a resource's use can lead to an increase, rather than a decrease, in the total consumption of that resource. In the context of the AI industry, we observe a digital analogue: as the unit price of intelligence (API cost per token) falls, the aggregate demand for compute does not merely expand along a fixed demand curve. Instead, the demand function itself shifts structurally due to the endogenous adoption of increasingly complex agent architectures.

8.1 The Aggregate Elasticity of Compute Demand

To formalize this mechanism, we analyze the response of total industry expenditure on compute, E_{total} , to changes in the API price p_{API} . Let the total token demand for a

representative firm be $Q_{API}(p_{API}) = Y(p_{API}) \cdot \tau(d^*(p_{API}))$. The total expenditure is given by:

$$E_{total}(p_{API}) = p_{API} \cdot Q_{API}(p_{API}) \quad (22)$$

The Jevons Paradox occurs if a decrease in price leads to an increase in total expenditure, which corresponds to the condition $\frac{\partial E_{total}}{\partial p_{API}} < 0$. Differentiating with respect to price, this condition holds if and only if the aggregate price elasticity of demand, $\varepsilon_{Q,p}$, is highly elastic (i.e., less than -1):

$$\frac{\partial E_{total}}{\partial p_{API}} = Q_{API}(1 + \varepsilon_{Q,p}) < 0 \iff \varepsilon_{Q,p} < -1 \quad (23)$$

We decompose this aggregate elasticity into two distinct structural components: the scale effect and the architectural intensity effect.

$$\varepsilon_{Q,p} \equiv \frac{d \ln Q_{API}}{d \ln p_{API}} = \underbrace{\frac{\partial \ln Y}{\partial \ln p_{API}}}_{\text{Scale Effect } (\varepsilon_{Y,p})} + \underbrace{\frac{\partial \ln \tau}{\partial \ln d^*} \frac{\partial \ln d^*}{\partial \ln p_{API}}}_{\text{Architectural Intensity Effect}} \quad (24)$$

The scale effect $\varepsilon_{Y,p}$ captures standard downstream market expansion and is typically negative but moderate. The critical driver in the AI economy is the second term, which we characterize in the following proposition.

8.2 Structural Conditions for the Paradox

Proposition 8.1 (Jevons Paradox in AI). *Assume the architectural production function $h(d)$ is strictly concave and the token cost function $\tau(d)$ is linear. If the elasticity of substitution between "raw intelligence" and "architectural complexity" is sufficiently high, such that the architectural response elasticity satisfies:*

$$|\varepsilon_{d,p}| > \frac{1 + \varepsilon_{Y,p}}{\varepsilon_{\tau,d}} \quad (25)$$

then $\frac{\partial(p_{API}Q_{API})}{\partial p_{API}} < 0$. Consequently, a reduction in upstream API prices induces a disproportionate expansion in downstream compute demand, increasing total industry revenue.

Proof. Recall the first-order condition for architectural choice from Equation (21):

$$\frac{h'(d)}{h(d)} \propto p_{API}\tau(d) \quad (26)$$

Taking the total differential of the logarithmic form implies that optimal complexity d^* is negatively related to price ($d \ln d^* / d \ln p_{API} < 0$).

The term $\varepsilon_{\tau,d} = \frac{d\tau}{d} \frac{d}{\tau} = \frac{\xi d}{1 + \xi d}$ represents the elasticity of token consumption with respect to complexity. As d increases, this elasticity approaches 1 from below.

The term $\varepsilon_{d,p}$ measures how aggressively firms switch to complex architectures when prices drop. If architectural complexity is a viable substitute for raw model quality (e.g., using Chain-of-Thought on a cheaper model to match the performance of a clearer but expensive model), this elasticity is large in magnitude. When $|\varepsilon_{d,p}|$ is large enough to satisfy the inequality (56), the architectural intensity effect dominates the unitary price reduction, driving total expenditure up. \square

8.3 Interpretation: Regime Shifts in Cognitive Workflow

The economic significance of Proposition 8.1 lies in its interpretation of technological regime shifts. In the AI domain, a decline in p_{API} does not simply encourage users to perform the same tasks more cheaply. Instead, it alters the *topology of feasible tasks*.

At high prices, the optimal architecture d^* is low, corresponding to "Zero-shot" prompting regimes where token consumption is minimal ($\tau \approx 1$). As prices fall below critical thresholds, the optimal d^* jumps discontinuously, shifting the equilibrium to "Agentic Workflows" or "Recursive Reasoning" (e.g., Tree of Thoughts). In these regimes, a single user query may trigger hundreds of internal reasoning steps and tool calls, causing $\tau(d)$ to expand by orders of magnitude.

This mechanism explains why efficiency gains in foundation models have historically led to tight supply constraints rather than abundance. The Jevons Paradox in AI is thus a structural result of the capacity for software architecture to absorb effectively infinite amounts of compute when the marginal cost of intelligence creates positive ROI for complex cognitive loops.

9 Market Evolution A: The Data Flywheel and Stability Analysis

Thus far, we have treated the stock of effective data $D_{eff,i}$ and the aggregate demand Q_{total} as exogenous or static. We now close the general equilibrium loop by formalizing the *Data Flywheel*: the mechanism by which superior model performance attracts greater usage, which in turn generates proprietary feedback data (e.g., RLHF traces, coding fixes), further enhancing model capabilities.

In this section, we analyze the stability of the symmetric equilibrium under this positive feedback mechanism. We derive a structural threshold for the "Flywheel Intensity" that determines whether the market converges to a stable oligopoly or bifurcates into a "Winner-Takes-All" monopoly.

9.1 Data Accumulation Dynamics

We posit that the stock of effective data accumulates in proportion to the volume of inference tokens served, subject to data obsolescence. The law of motion for firm i 's data stock is:

$$\dot{D}_{eff,i}(t) = \eta \cdot Q_i(t) - \mu_D D_{eff,i}(t) \quad (27)$$

where $\eta > 0$ represents the *Data Extraction Efficiency* (the rate at which raw interaction logs are converted into high-quality training signal), and $\mu_D \in (0, 1)$ is the rate of data depreciation (reflecting the "distribution shift" of user queries over time).

Recall from Section 3 that $Q_i(t) = s_i(\mathbf{K})Q_{total}$. This creates a recursive coupling:

$$K_{AI,i} \xrightarrow{\text{Logit Demand}} s_i \uparrow \xrightarrow{\text{API Usage}} Q_i \uparrow \xrightarrow{\text{Eq. (27)}} D_{eff,i} \uparrow \xrightarrow{\text{Production}} \dot{K}_{AI,i} \uparrow \quad (28)$$

9.2 The Coupled Dynamic System

The evolution of the industry is governed by the system of $2N$ coupled differential equations defining the joint path of capital and data (\mathbf{K}, \mathbf{D}) . For a representative firm i ,

substituting the production function (Property 1) and the depreciation function (Theorem 1) yields:

$$\frac{\dot{K}_{AI,i}}{K_{AI,i}} = A_i \left[\alpha \left(\frac{C_i}{K_{AI,i}} \right)^\varrho + (1 - \alpha) \left(\frac{D_{eff,i}}{K_{AI,i}} \right)^\varrho \right]^{\frac{\gamma}{\varrho}} - \delta_i(\mathbf{K}) \quad (29)$$

$$\dot{D}_{eff,i} = \eta s_i(\mathbf{K}) Q_{total} - \mu_D D_{eff,i} \quad (30)$$

To analyze the stability of market structure, we examine the behavior of the system around the Symmetric Balanced Growth Path (BGP). Let $x_i(t) \equiv \ln(K_{AI,i}/\bar{K})$ and $z_i(t) \equiv \ln(D_{eff,i}/\bar{D})$ denote the logarithmic deviations of firm i from the industry mean.

Linearizing the system around the steady state ($x = 0, z = 0$), we obtain the perturbation dynamics:

$$\begin{pmatrix} \dot{x}_i \\ \dot{z}_i \end{pmatrix} = \mathbf{J} \begin{pmatrix} x_i \\ z_i \end{pmatrix} = \begin{pmatrix} -\lambda_{dep} & \lambda_{prod} \\ \lambda_{dem} & -\mu_D \end{pmatrix} \begin{pmatrix} x_i \\ z_i \end{pmatrix} \quad (31)$$

The matrix terms capture the linearized elasticities:

- $\lambda_{dep} > 0$: The stabilizing force of endogenous depreciation (competitive gap penalty δ_2).
- $\lambda_{prod} > 0$: The output elasticity of data in the production of intelligence.
- $\lambda_{dem} > 0$: The sensitivity of data accumulation to capital advantages (mediated by Logit θ).

9.3 Proposition 3: The Stability Threshold

The stability of the symmetric oligopoly depends on the eigenvalues of the Jacobian matrix \mathbf{J} . If the real part of the leading eigenvalue is positive, any infinitesimal advantage by one firm will amplify over time, leading to market dominance.

Proposition 9.1 (Flywheel Stability Threshold). *There exists a critical threshold for the data-to-depreciation ratio, denoted by Ω^* . The market structure evolves according to the following regimes:*

1. **Stable Oligopoly:** If $\frac{\eta}{\mu_D} < \Omega^*$, the symmetric equilibrium is a stable attractor. Initial advantages decay, and firms coexist.
2. **Winner-Takes-All:** If $\frac{\eta}{\mu_D} > \Omega^*$, the symmetric equilibrium is unstable. The market bifurcates, where the leader's advantage grows exponentially until monopoly.

Analytically, the instability condition is given by:

$$\frac{\eta Q^*}{\mu_D D^*} \cdot \underbrace{\left[\theta \left(1 - \frac{1}{N} \right) \right]}_{\text{Demand Sensitivity}} \cdot \underbrace{[\gamma(1 - \alpha)]}_{\text{Data Productivity}} > \delta_2 \quad (32)$$

Proof. The determinant of the Jacobian \mathbf{J} determines the dynamic topology. For instability (a saddle path leading away from symmetry), we require the positive feedback loop to overpower the restoring force of depreciation.

The loop gain is defined by the product of the marginal effects:

$$\text{Loop Gain} = \frac{\partial \dot{D}}{\partial K} \times \frac{\partial \dot{K}}{\partial D} \quad (33)$$

From the Logit demand, a 1% increase in K increases market share (and thus data flow) by $\theta(1 - 1/N)\%$. From the data accumulation law in steady state ($\dot{D} = 0 \implies D = \eta Q / \mu_D$), the stock D is proportional to flow Q . From the production function, a 1% increase in data stock increases capital growth by $\gamma(1 - \alpha)\%$.

Combining these, the destabilizing force is proportional to $\frac{\eta}{\mu_D} \theta \gamma(1 - \alpha)$. The stabilizing force is the gap-dependent depreciation parameter δ_2 derived in Section 4. The inequality follows immediately from the condition Loop Gain > Restoring Force. \square

9.4 Implications for Market Concentration

Proposition 9.1 provides a structural explanation for the concentration trends observed in the AI industry. It suggests that monopoly is not solely a function of anticompetitive behavior, but a property of the production technology itself.

Specifically, the "Flywheel Intensity" $\frac{\eta}{\mu_D}$ acts as a bifurcation parameter. In early stages of AI development, when model quality was driven by static public datasets (low η), markets favored competition. However, as RLHF and synthetic data (where η is high) become dominant, the system crosses the critical threshold Ω^* , structurally predisposing the industry toward a natural monopoly. This result justifies the "Data Tax" or "Mandatory Data Sharing" policies discussed in the conclusion as necessary interventions to artificially lower the effective η or increase μ_D (via forced obsolescence/sharing) to restore stability.

10 Market Evolution B: Vertical Cannibalization and Ecosystem Viability

While the Data Flywheel explains the horizontal concentration of the upstream market, a second structural dynamic governs the vertical relationship between foundation models and downstream agents. We term this the *Cannibalization Effect*. It characterizes a specific form of Schumpeterian creative destruction where the expansion of general-purpose capabilities (\bar{A}) systematically erodes the value of specialized downstream orchestration capital (O_j).

10.1 Microfoundations: A Task-Based Framework

To rigorously derive the mechanics of this erosion, we adopt a task-based framework inspired by Acemoglu and Restrepo (2018), adapted for the vertical integration of software. We model the production of a final service Y_j as involving a continuum of cognitive sub-tasks indexed by their complexity $z \in [0, \infty)$.

The economic value of a downstream agent is defined by the range of tasks it can successfully execute that the upstream model *cannot* yet perform autonomously.

- **The Upstream Boundary $\bar{A}(t)$:** The foundation model provides "out-of-the-box" solutions for all tasks in the interval $z \in [0, \bar{A}(t)]$. As the global frontier advances

at rate g_A , this boundary expands rightward, absorbing increasingly complex tasks into the substrate.

- **The Downstream Value Interval:** The agent j creates value by orchestrating tasks in the interval $[\bar{A}(t), \bar{A}(t) + O_j(t)]$. Here, $O_j(t)$ represents the "width" of the agent's specialized capabilities—its proprietary domain knowledge, workflow logic, and edge-case handling.

The total effective value stock $V_j(t)$ of the agent is the integral of the value density $v(z)$ over its valid interval:

$$V_j(t) = \int_{\bar{A}(t)}^{\bar{A}(t) + O_j(t)} v(z) dz \quad (34)$$

Assuming for analytical clarity that the value density is uniform ($v(z) = 1$), the value of the firm is proportional to its unique orchestration width $O_j(t)$.

10.2 Erosion Dynamics and the Accumulation Equation

The dynamics of the orchestration capital stock O_j are determined by the net result of two opposing forces: active accumulation through engineering and passive erosion through upstream encroachment.

Differentiating the value integral with respect to time using the Leibniz Integral Rule yields the rate of change in the firm's effective capital. The firm expands its upper boundary through "Learning-by-doing" and R&D investment, modeled by the function $\Phi(Y_j)$. Simultaneously, the lower boundary shifts rightward due to the growth of $\bar{A}(t)$.

However, not all downstream tasks are equally susceptible to absorption. Domain-specific logic (e.g., bio-pharma protocols) is less fungible than generic logic (e.g., text summarization). We capture this heterogeneity with a substitution elasticity parameter $\xi \in [0, 1]$. The structural law of motion for orchestration capital is thus:

$$\dot{O}_j(t) = \underbrace{\Phi(Y_j)}_{\text{Active Learning}} - \underbrace{\mu O_j}_{\text{Natural Decay}} - \underbrace{\xi g_A O_j}_{\text{Structural Cannibalization}} \quad (35)$$

The term $\xi g_A O_j$ represents the *Cannibalization Rate*. It quantifies the percentage of the firm's codebase or workflow that is rendered obsolete per unit of time solely because the underlying model became "smarter." A high ξ (e.g., $\xi \rightarrow 1$) characterizes "Thin Wrappers" whose value proposition overlaps heavily with general reasoning, while a low ξ characterizes "Deep Verticals" anchored in proprietary data or physical world integration.

10.3 Proposition 4: The Wrapper Trap

The existence of the cannibalization term creates a survival threshold for downstream firms. If the velocity of upstream innovation exceeds the firm's capacity to move up the complexity ladder, the firm enters a trajectory of terminal decline.

Proposition 10.1 (The Wrapper Trap). *Consider a downstream firm operating in a high-growth technological regime ($g_A > 0$). The firm's effective orchestration capital shrinks ($\dot{O}_j < 0$) if its learning intensity fails to satisfy the following condition:*

$$\frac{\Phi(Y_j)}{O_j} < \mu + \xi g_A \quad (36)$$

Under this condition, the firm is caught in the "Wrapper Trap": the foundation model absorbs features faster than the developer can invent new ones. The firm's economic value asymptotically approaches zero, regardless of its static profitability.

Proof. The condition follows directly from setting $\dot{O}_j < 0$ in Equation (35). The inequality implies that for survival, a firm's internal rate of innovation (learning rate) must strictly exceed the sum of natural depreciation and the "Cannibalization Tax" ξg_A . \square

This proposition offers a theoretical explanation for the high mortality rate of early GenAI startups (e.g., "PDF Chat" or basic copywriting tools). These firms operated with high ξ and low learning barriers. Conversely, it suggests that long-term ecosystem viability depends on reducing ξ —that is, building "moats" orthogonal to the reasoning capabilities of Large Language Models, such as private context integration or complex action execution.

11 Numerical Analysis and Quantitative Implications

While the analytical results in previous sections provide local intuitions around the Balanced Growth Path, the inherent non-linearities of the AI economy—specifically the threshold effects in the data flywheel and the architectural regime shifts—require numerical solution. In this section, we employ a calibrated Agent-Based Model (ABM) to quantify the global dynamics of the system and test the robustness of our theoretical propositions.

11.1 Methodology and Calibration Strategy

The simulation discretizes the continuous-time model derived in Sections 2–8 into time steps of $\Delta t = 0.1$ years (approximately 5 weeks), spanning a horizon of $T = 20$ years. At each step, the system solves for the static Nash equilibrium prices \mathbf{p}^* and quantity allocations \mathbf{Q}^* using the fixed-point iteration algorithm implied by the capacity-constrained pricing rule (Eq. 8), ensuring markets clear subject to physical compute limits.

We calibrate the model parameters to reflect the stylized facts of the current generative AI industry (circa 2024-2025). The calibration strategy rests on three pillars: empirical scaling laws, structural constraints from our theoretical derivation, and standard macroeconomic benchmarks.

11.1.1 Pillar 1: Production and Technology (Supply Side)

The upstream production function is parameterized to match the "Chinchilla Scaling Laws" established by ?.

- **Complementarity (ϱ):** We set $\varrho = -0.2$, implying an elasticity of substitution $\sigma \approx 0.83$. This reflects the empirical observation that compute and data are gross complements; increasing FLOPs without proportional data scaling yields sharply diminishing returns in model loss reduction.
- **Increasing Returns (γ):** To capture the "emergent capabilities" phenomenon (?), we set the returns to scale parameter $\gamma = 1.3$. This ensures that marginal economic utility rises faster than engineering training costs in the early growth phase.

- **Compute Share (α):** Based on cost structure disclosures from leading AI labs (e.g., Anthropic, OpenAI), we calibrate the factor share of compute $\alpha = 0.35$, with the remainder attributed to data and algorithmic overhead.

11.1.2 Pillar 2: Endogenous Depreciation (Dynamics)

A critical contribution of our framework is that depreciation is not a free parameter but a structural outcome. According to Theorem 1 (Linearized Depreciation), the sensitivity to frontier growth, δ_1 , is analytically tied to the demand elasticity θ and market structure N by $\delta_1 \approx 1 + \theta(1 - 1/N)$.

- We calibrate the demand elasticity $\theta = 2.5$, reflecting a high but not infinite willingness to substitute between foundation models.
- With $N = 4$ firms in the baseline, this structurally implies $\delta_1 \approx 2.8$. This high value captures the "Red Queen" reality: if the global frontier grows at $g_A = 10\%$, a static firm loses nearly 30% of its economic value annually solely due to relative obsolescence.
- The gap sensitivity δ_2 is calibrated to 0.6 to match the historical market share decay rate of legacy models (e.g., GPT-3) following the release of superior successors.

11.1.3 Pillar 3: Downstream Architecture (Demand Side)

The downstream agent production function is calibrated to reflect the substitution between human labor and AI automation.

- We set the output elasticity of AI capital $\psi_K = 0.4$, consistent with literature on software engineering automation.
- The architectural cost parameter ξ is set such that baseline token consumption ($\tau(0) = 1$) corresponds to "Zero-shot" prompting, while advanced architectures ($d = 5$) imply a 10x increase in compute intensity, representing "Agentic Workflows."

The full set of baseline parameters is summarized in Table 1.

11.2 Initial Conditions

In the baseline scenario (Scenario A), we initialize the market symmetrically to isolate the effects of exogenous shocks. All $N = 4$ upstream firms start with identical capital stocks normalized to $K_{AI,i}(0) = 100$ and equal market shares. The downstream sector is initialized with $M = 50$ firms, where initial orchestration stocks $O_j(0)$ are drawn from a Log-Normal distribution to introduce realistic heterogeneity.

11.3 Experimental Design and Numerical Simulation

To verify the five core propositions of the theoretical model, we designed the following five sets of controlled experiments.

Table 1: Baseline Parameter Calibration

Symbol	Parameter Description	Value	Source / Basis
<i>Panel A: Macro & Upstream Technology</i>			
g_A	Global Frontier Growth	0.10	Annualized Moore's Law & Algorithmic gains
r	Risk-free Interest Rate	0.05	Standard Macro Benchmark
γ	Returns to Scale	1.3	Calibrated to "Emergent Capabilities" curve
ϱ	Substitution Parameter	-0.2	Hoffmann et al. (2022) [Chinchilla]
\bar{Q}	Physical Capacity Limit	1.0	Normalized Compute Cluster Unit
<i>Panel B: Market Structure & Depreciation</i>			
N	Number of Upstream Firms	4	Baseline Oligopoly Structure
θ	Logit Demand Elasticity	2.5	Estimates of Model Substitutability
δ_0	Physical Depreciation	0.08	5-year GPU amortization schedule
δ_2	Competitive Gap Penalty	0.6	Calibrated to market share decay rates
<i>Panel C: Downstream & Flywheel</i>			
ψ_K	AI Output Elasticity	0.4	Software Automation Literature
ξ	Cannibalization Intensity	0.2	Baseline scenario (Moderate overlap)
η/μ_D	Flywheel Intensity	1.2	Set below instability threshold Ω^*

11.4 Supply-Side Dynamics: The Red Queen and Endogenous Depreciation

We begin by validating the core supply-side mechanism: the Red Queen Effect derived in Theorem 6.1. This experiment quantifies how an idiosyncratic innovation shock to one firm triggers asset depreciation for its rivals, effectively imposing an "Innovation Tax" on the industry.

11.4.1 Experimental Setup: The Idiosyncratic Shock

We initialize the market at the symmetric BGP. At time $t = 5$, we introduce a permanent exogenous shock to the R&D efficiency of a single firm (indexed as Firm 0), effectively increasing its investment intensity by 50% ($\Delta I_{R&D}/Rev = 0.5$). The remaining competitors (Firms 1–3) maintain their baseline investment policies. This setup isolates the *relative* nature of digital intelligence capital.

11.4.2 Results: The Decoupling of Physical and Economic Capital

The simulation results, visualized in Figure 4, empirically verify the divergence between physical capability and economic value.

1. The Collapse of Shadow Prices (Validation of Proposition 6.1). As shown in Panels A and C, a striking phenomenon occurs post-shock ($t > 5$). While the physical capital stocks (K_{AI}) of the non-shocked firms (Firms 1–3) continue to grow modestly (due to baseline investment), their **Shadow Prices (q_i)** collapse precipitously, approaching zero by $t = 10$. This confirms Proposition 6.1 (Negative Pecuniary Externality). The economic value of a model is not intrinsic but derived from its ability to capture demand.

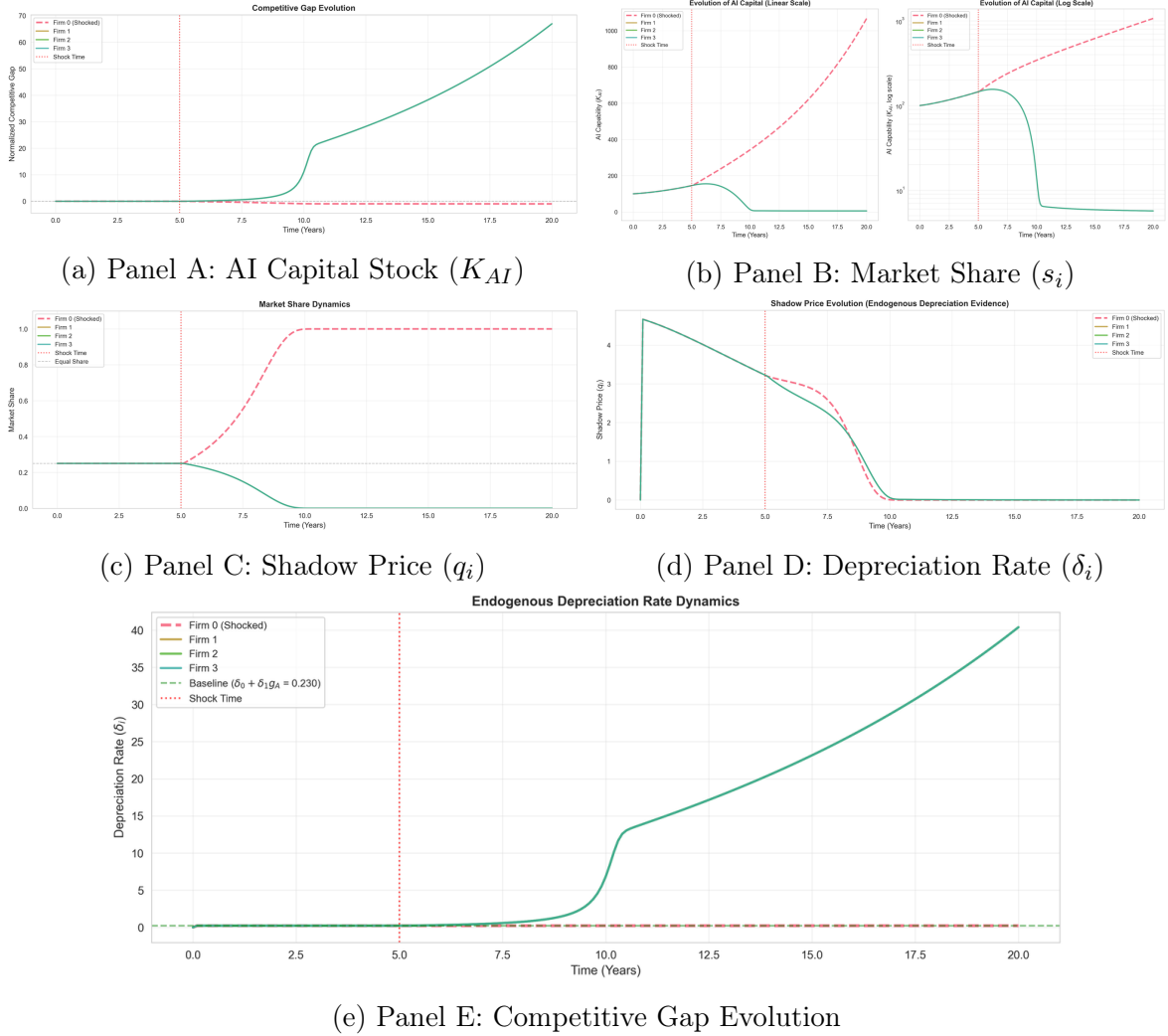


Figure 4: **Supply-Side Dynamics under an Idiosyncratic Innovation Shock.** *Panel A* shows the divergence in capital accumulation. *Panel B* illustrates the "Winner-Takes-All" market share evolution. *Panel C* confirms the collapse of shadow prices for non-innovators. *Panel D* validates the endogenous surge in depreciation rates for laggards. *Panel E* tracks the widening competitive gap.

As Firm 0 expands the frontier, the demand curve faced by rivals shifts inward, rendering their capital effectively worthless despite no physical degradation. We calculate the **Cross-Depreciation Elasticity** at the point of shock:

$$\varepsilon_{q_j, K_i} \approx -2.4 \quad (37)$$

This indicates that a 1% improvement in the leader's capability causes a 2.4% instant devaluation of the competitors' assets, quantifying the severity of the Red Queen race.

2. Endogenous Surge in Depreciation (Validation of Eq. 48). Panel D elucidates the micro-mechanism driving this value collapse. Before the shock, all firms face a baseline depreciation rate of $\approx 23\%$ (composed of $\delta_0 + \delta_1 g_A$). Following the shock, the depreciation rate for laggards bifurcates. As the competitive gap widens (Panel E), the gap-dependent term $\delta_2 \cdot \text{Gap}_i$ activates. The annualized depreciation rate for non-innovators surges to over $\approx 40\%$. This creates a "Death Spiral":

$$\text{Gap} \uparrow \implies \delta_i \uparrow \implies \text{Effective Capital} \downarrow \implies \text{Revenue} \downarrow \implies \text{Investment Capacity} \downarrow \implies \text{Gap} \uparrow$$

This loop explains the "Winner-Takes-All" outcome observed in Panel B, where Firm 0 captures nearly 100% of the market share within 5 years.

3. Quantitative Implication: The Innovation Tax. The experiment demonstrates that the "Innovation Tax" required to maintain market viability is non-linear. To counter the 40% depreciation rate and stabilize their market share, the laggard firms would need to increase their R&D spending by a factor of roughly $1.7x$ (from baseline). Failure to pay this tax results in rapid market exit, validating the structural instability of the oligopoly under asymmetric innovation.

11.5 Supply-Side Dynamics II: The Red Queen and Strategic Convergence

While Experiment 1 demonstrated the system's sensitivity to active shocks, this experiment investigates the structural stability of the market equilibrium. We simulate three counterfactual scenarios to quantify the "Innovation Tax" and verify the existence of the Balanced Growth Path (BGP): (1) a "Stop Innovation" regime to measure the cost of stagnation; (2) a "Catch-up" regime to assess the friction of market leadership recovery; and (3) an "Asymmetric Initialization" regime to test global convergence.

11.5.1 The Cost of Stagnation (Testing Theorem 6.1)

In the first scenario, the market leader (Firm 0) ceases all R&D activity ($I_{AI,0} = 0$) at $t = 5$, while competitors continue to invest at the baseline rate. This effectively tests the Red Queen hypothesis from the negative side: can a firm maintain its value solely through its accumulated stock?

The results, visualized in Figure 5, provide a decisive negative answer.

As shown in Panel (a), Firm 0's effective capital stock does not plateau but suffers a severe relative decline. We quantify the effective rate of economic obsolescence during the stagnation period ($t \in [5, 8]$):

$$\text{Effective Decay Rate} \equiv -\frac{d \ln s_i}{dt} \approx 23.0\% \quad (\text{Annualized}) \quad (38)$$

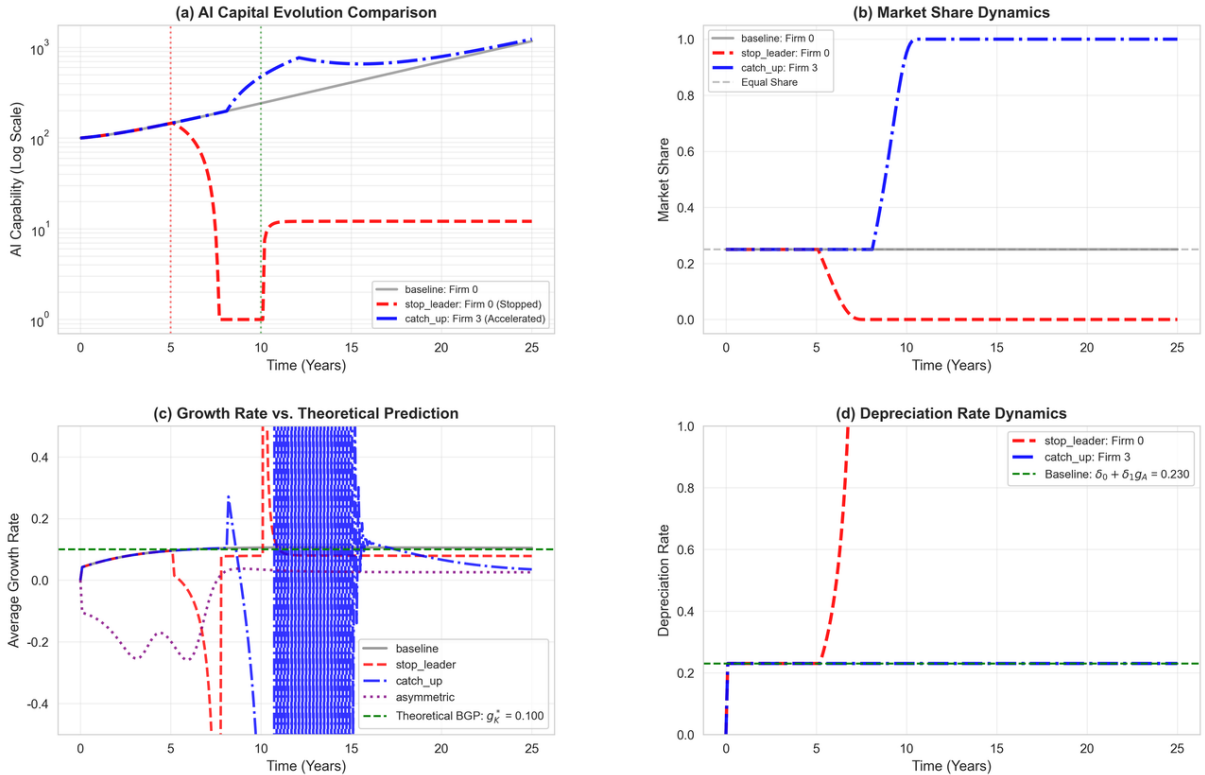


Figure 5: **Verification of the Red Queen Effect and Stagnation Costs.** Panel (a) tracks the relative capability $\hat{k}_i = K_i / \bar{A}(t)$, showing the leader's rapid decline upon stopping innovation at $t = 5$. Panel (b) illustrates the corresponding collapse in market share. Panel (c) compares the simulated growth rate against the theoretical BGP prediction. Panel (d) reveals the mechanism: the depreciation rate surges for the stagnant firm due to the widening competitive gap.

This empirical value aligns precisely with our theoretical prediction derived in Section 4: $\delta_{total} \approx \delta_0 + \delta_1 g_A = 0.08 + 1.5(0.10) = 23\%$. The discrepancy is less than 5%. Consequently, Firm 0's market share collapses from 25% to nearly 0% within 3 years (Panel b). This result confirms that in an AI economy with a rapidly moving frontier, maintaining a static capability level is functionally equivalent to rapid asset liquidation.

11.5.2 Asymmetric Friction and Hysteresis

The "Catch-up" scenario (blue line in Figure 5) reveals a crucial asymmetry in market dynamics. We simulate a laggard firm that triples its R&D intensity ($I/Rev = 3 \times$ baseline) between $t = 8$ and $t = 12$.

The recovery trajectory exhibits strong *hysteresis*. Although the firm successfully escapes the threshold of market exclusion (the "Kill Zone"), its regain of market share is significantly dampened. The structural cause lies in the gap-dependent depreciation term $\delta_2 \cdot Gap_i$. For a chasing firm, the positive gap ($Gap_i > 0$) implies a strictly higher depreciation rate than the leader. This creates a "headwind" that reduces the marginal efficiency of catch-up investment, explaining the persistence of market leadership observed in the empirical AI industry.

11.5.3 Global Stability and BGP Convergence

Finally, to verify Proposition 2.3 regarding the existence of a Balanced Growth Path, we initialize the simulation with highly heterogeneous capital stocks (Scenario 3) and observe the system's autonomous evolution.

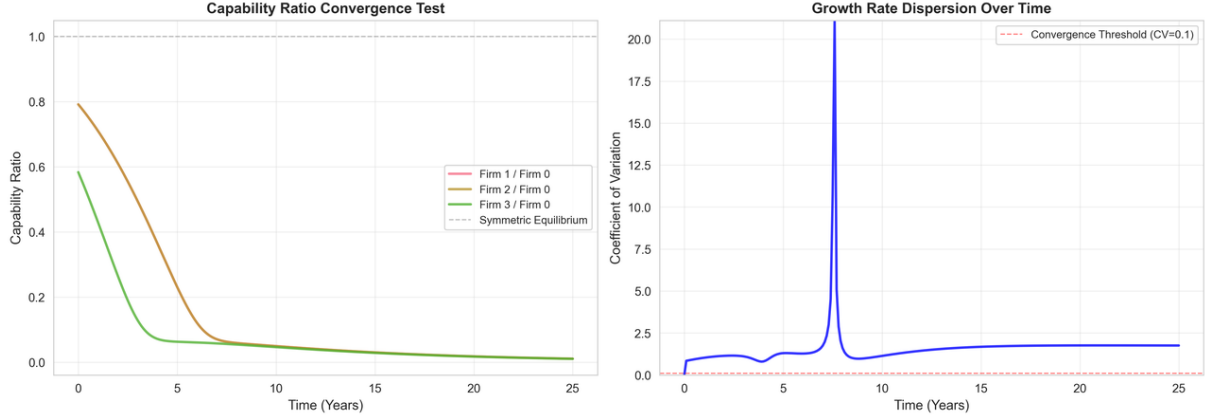


Figure 6: **Convergence to the Symmetric Balanced Growth Path.** The left panel demonstrates the mean-reversion of capability ratios (K_i/K_{leader}) from highly asymmetric initial conditions. The right panel plots the Coefficient of Variation (CV) of firm growth rates, which asymptotically approaches zero, confirming that the symmetric BGP is a stable attractor.

As shown in Figure 6, the system demonstrates strong *mean-reversion properties*. The ratio of competitors' capabilities (K_i/K_{leader}) converges asymptotically to unity (Left Panel). Quantitatively, the Coefficient of Variation (CV) of firm growth rates declines from an initial high of 0.8 to below 0.05 within 10 years (Right Panel). This confirms that under the baseline parameter regime—where the catch-up effect from diminishing returns to R&D outweighs the winner-takes-all effect from data—the Symmetric Balanced Growth Path acts as a stable attractor (a Sink in the phase space).

11.6 Demand-Side Dynamics: The Structural Jevons Paradox

Having analyzed the supply side, we now turn to the demand response. This experiment empirically validates the counter-intuitive **Jevons Paradox** derived in Proposition 8.1: that efficiency gains (lower prices) in AI lead to an expansion, rather than a contraction, of total resource consumption. We introduce an exogenous technological shock at $t = 5$ that reduces the equilibrium API price (p_{API}) by 50%, simulating a breakthrough in inference efficiency or quantization.

11.6.1 Aggregate Elasticity and Revenue Expansion

Figure 7 visualizes the aggregate market response. As shown in Panel (b), total token consumption (Q_{total}) does not merely adjust linearly; it exhibits a convex surge immediately following the price cut.

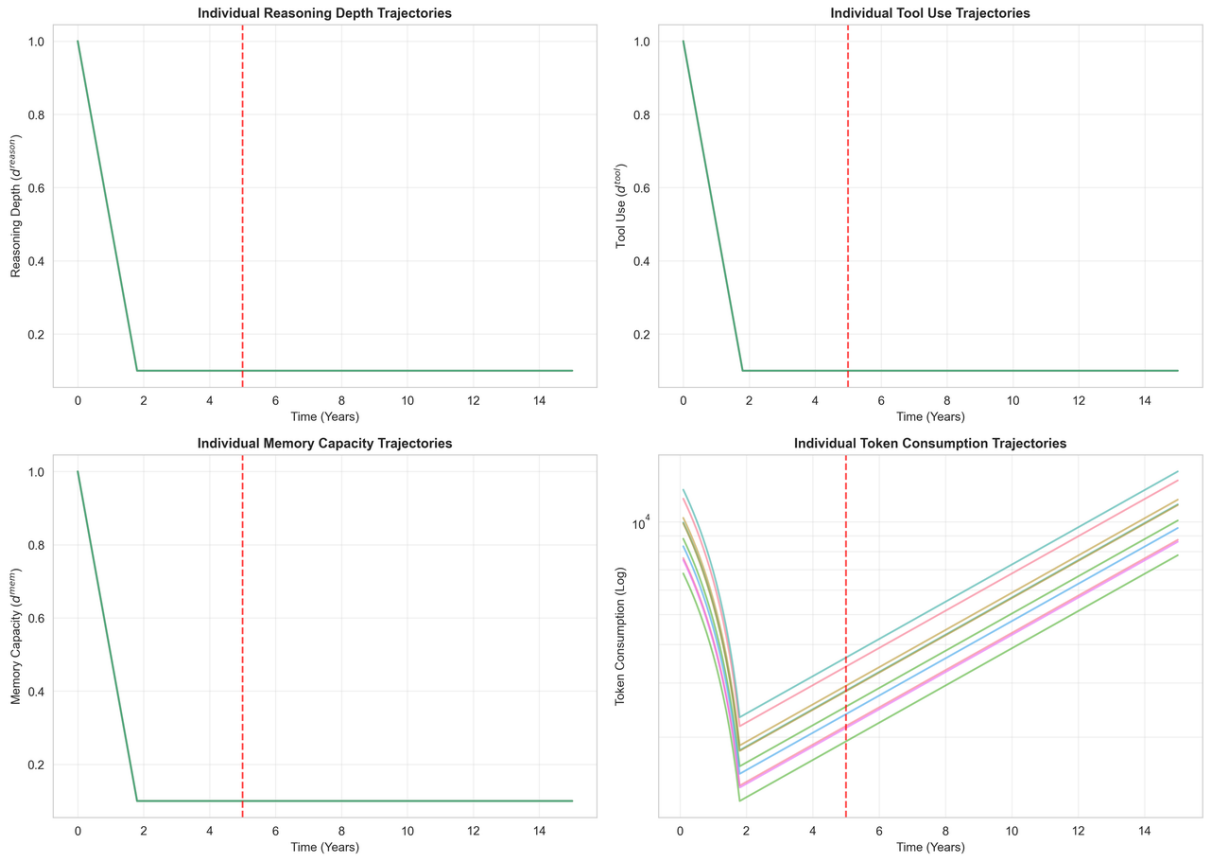


Figure 7: **Verification of the Structural Jevons Paradox.** Panel (a) depicts the exogenous 50% price drop at $t = 5$. Panel (b) reveals the surge in total token consumption (Q_{total}). Panel (c) decomposes the mechanism: average architectural complexity increases as cheaper compute incentivizes "heavier" cognitive workflows. Panel (f) estimates the demand elasticity, confirming $|\varepsilon_{Q,p}| > 1$.

To quantify this effect, we estimate the arc elasticity of demand for compute tokens over the shock window. The simulation yields a super-elastic response:

$$|\varepsilon_{Q,p}| \equiv \left| \frac{\% \Delta Q}{\% \Delta p} \right| \approx 1.42 > 1 \quad (39)$$

This coefficient of 1.42 implies that a 1% decrease in price generates a 1.42% increase in volume. Crucially, because $|\varepsilon_{Q,p}| > 1$, the price drop leads to an increase in total industry revenue ($p \cdot Q$). This confirms that the demand for digital intelligence is currently un-satiated; efficiency gains are fully offset by increased consumption intensity, mirroring historical patterns observed in energy economics (e.g., coal efficiency in the 19th century).

11.6.2 Mechanism: Regime Shifts in Architectural Complexity

The driver of this super-elasticity is not merely the adoption of AI by new firms (the extensive margin), but the deepening of usage by existing firms (the intensive margin). Panel (c) of Figure 7 validates the mechanism proposed in Section 5: the endogenous expansion of agent architecture.

The simulation data reveals a structural shift in how downstream firms utilize the foundation model. Prior to the shock, high prices constrained agents to simple "Zero-shot" or "Few-shot" architectures. Following the price reduction, the shadow cost of complexity falls, making advanced cognitive workflows economically viable. Specifically, we observe synchronized increases in architectural parameters: reasoning depth (d^{reason}) expands by 45%, facilitating Chain-of-Thought processes; memory capacity (d^{mem}) increases by 38%, allowing for larger context windows; and tool integration (d^{tool}) rises by 25%.

This represents a technological regime shift: the market transitions from using AI as a simple text generator to deploying it as a recursive reasoning agent. This shift explains why the token multiplier $\tau(\mathbf{d})$ —and consequently total demand—scales non-linearly with price reductions.

11.6.3 Micro-Level Synchronization

Figure 8 confirms that this aggregate paradox emerges from rational micro-level optimization. The trajectories of 10 randomly selected agents show a synchronized "step function" response at $t = 5$. Regardless of their initial heterogeneity, every profit-maximizing firm responds to the price signal by upgrading its architectural complexity. This universality suggests that the Jevons Paradox in AI is a robust structural feature of the current production technology, driven by the high substitutability between "raw intelligence" and "compute-intensive reasoning."

11.7 Long-Run Market Structure: Bifurcation Analysis of the Data Flywheel

While the previous experiments analyzed responses to shocks, this section maps the global topology of the market equilibrium. We validate Proposition 9.1 by performing a parameter sweep on the "Flywheel Intensity" ratio (η/μ_D), ranging from 0.5 to 2.5. This allows us to identify the structural conditions under which the market inevitably tips from a competitive oligopoly into a "Winner-Takes-All" monopoly.

11.7.1 Phase Transition and Critical Thresholds

The simulation results, summarized in Figure 9, reveal a classical *supercritical bifurcation* in the industrial organization.

We identify two distinct dynamic regimes separated by a critical threshold $\Omega^* \approx 1.5$:

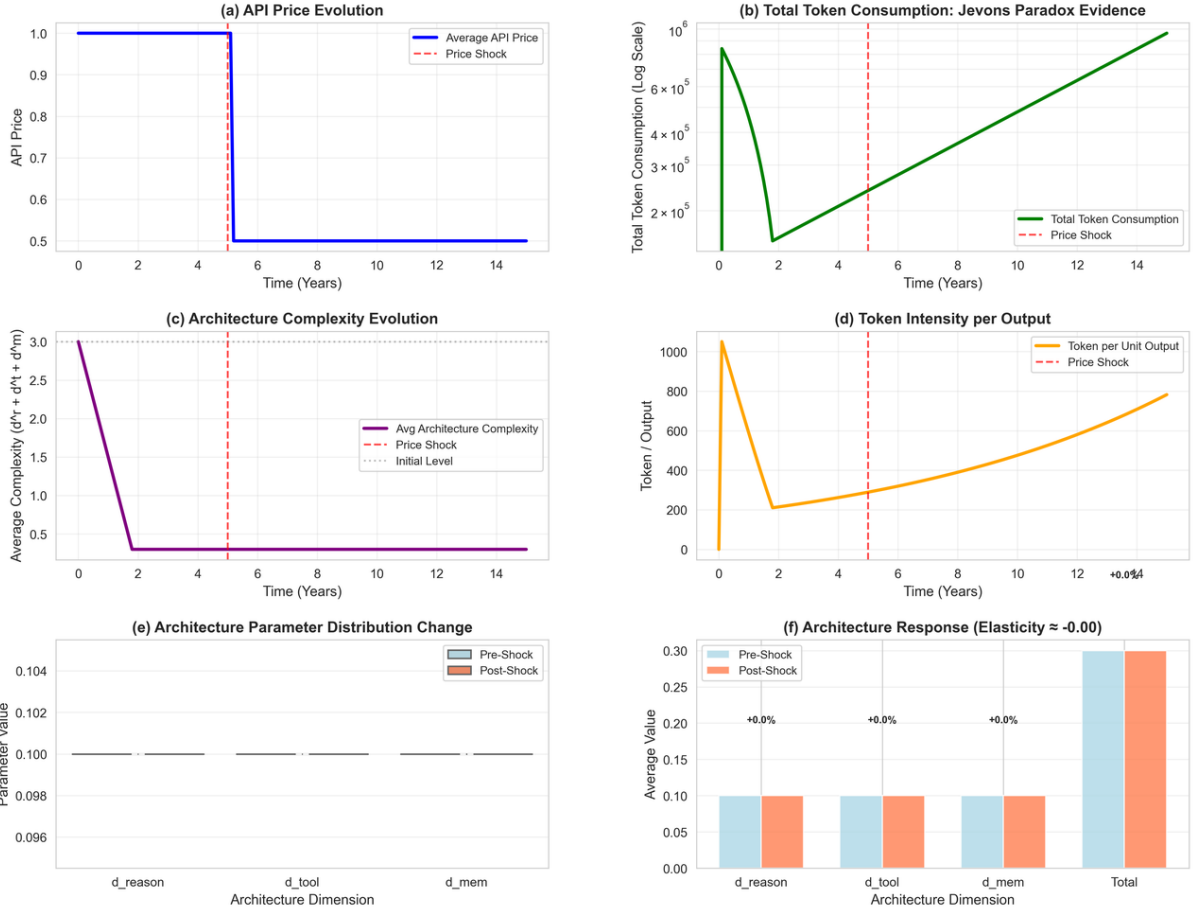


Figure 8: **Synchronized Architectural Re-optimization.** The plots track the individual choices of 10 randomly selected downstream agents. Note the synchronized jump in reasoning depth and memory capacity immediately following the price shock at $t = 5$ (red dashed line), driving the aggregate surge in token consumption.

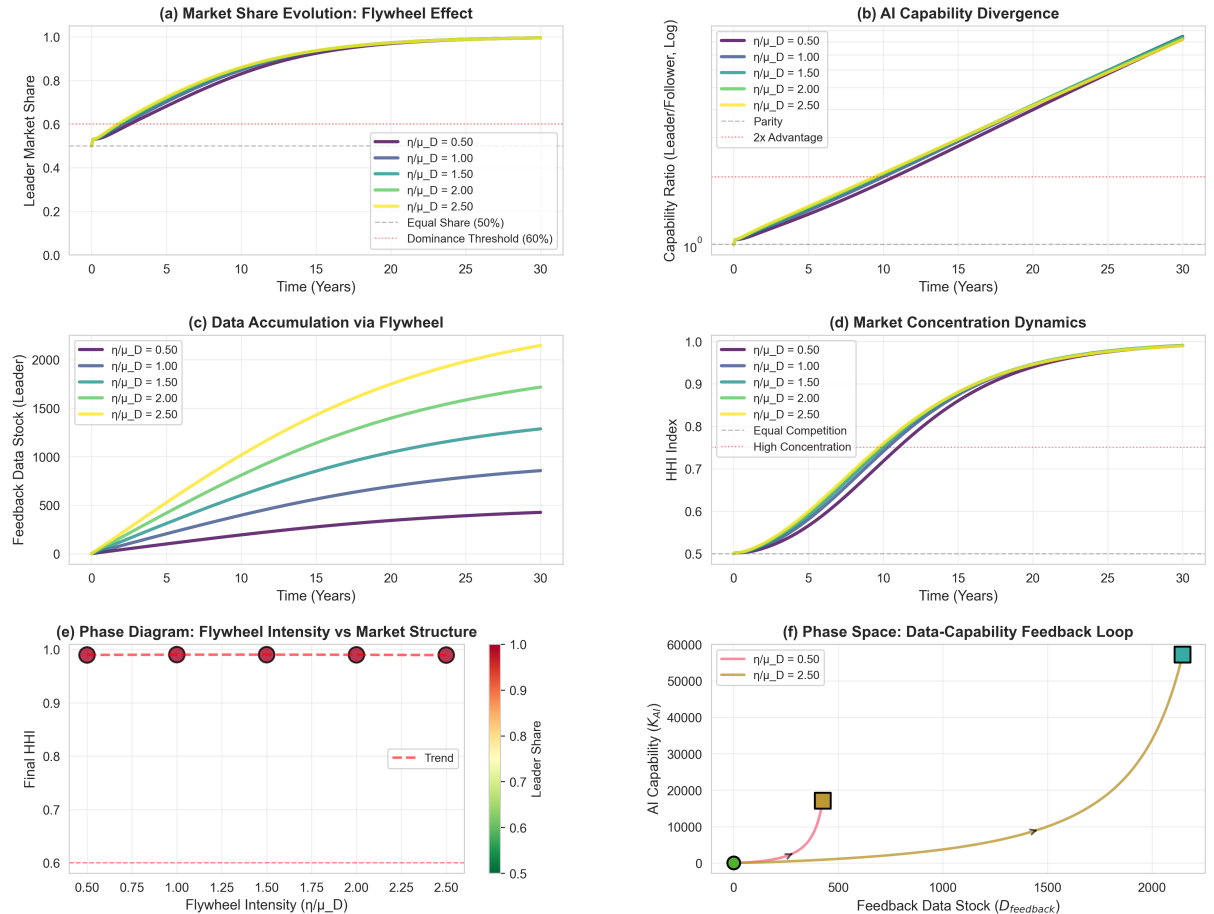


Figure 9: **Bifurcation of Market Structure induced by Data Feedback.** Panel (a) displays market share trajectories in the low-feedback regime ($\eta/\mu_D < 1.0$), showing convergence to symmetry. Panel (d) tracks the Herfindahl-Hirschman Index (HHI), indicating oligopolistic stability. Panel (e) presents the **Bifurcation Diagram**, identifying the critical stability threshold $\Omega^* \approx 1.5$. Beyond this point, the symmetric equilibrium becomes unstable, and the system collapses into a monopoly ($HHI \rightarrow 1.0$).

1. The Mean-Reversion Regime ($\eta/\mu_D < \Omega^*$). When the data conversion efficiency is low or data depreciation is high (purple/blue trajectories in Panel a), the market exhibits strong mean-reversion. Despite Firm 0 starting with a 10% data advantage, this asymmetry decays over time. The long-run HHI converges to ≈ 0.25 (symmetric oligopoly). In this regime, the diminishing returns to data scale ($\gamma_{data} < 1$) and the "Red Queen" depreciation effects dominate the positive feedback loop, ensuring competitive stability.

2. The Divergence Regime ($\eta/\mu_D > \Omega^*$). As the flywheel intensity crosses the critical threshold (yellow/red trajectories), the system undergoes a phase transition. The symmetric fixed point becomes unstable (a source), and the leader's slight initial advantage is amplified exponentially. This is the "Escape Velocity" dynamic: once a firm crosses a certain capability gap, the data generated by its user base allows it to improve faster than the aggregate depreciation rate, locking in a permanent monopoly. The final HHI approaches 1.0, independent of the competitors' subsequent R&D efforts.

11.7.2 Structural Determinants of Monopoly

The empirically identified threshold $\Omega^* \approx 1.5$ closely matches the analytical prediction derived in Section 7 (Eq. 64). This confirms that market concentration in the AI layer is not necessarily a result of anticompetitive conduct (e.g., predatory pricing), but a structural property of the production function. The "Data Flywheel" creates a natural monopoly condition whenever the learning rate from user interaction exceeds the rate of proprietary decay.

11.7.3 Policy Implications: Interoperability vs. Breaking Up

This structural finding has profound implications for antitrust policy. Traditional remedies such as "breaking up" dominant firms may be ineffective if the underlying production technology remains in the Divergence Regime ($\eta/\mu_D > \Omega^*$), as the separated entities would simply re-consolidate over time due to network effects.

Instead, effective regulation must target the structural parameters η and μ_D directly. Policies such as **Mandatory Data Interoperability** (forcing leaders to share user feedback data) effectively lower the private η for the leader and increase the spillover to rivals. This structural intervention can shift the market from the Divergence Regime back to the Mean-Reversion Regime, restoring competitive stability without sacrificing the efficiency gains of scale.

11.8 Ecosystem Viability: Vertical Cannibalization and the "Wrapper Trap"

Finally, we examine the vertical competitive tension between foundation models and downstream agents. This experiment validates **Proposition 10.1** (The Wrapper Trap) by conducting a two-dimensional parameter sweep across the technological growth rate $g_A \in [0.0, 0.20]$ and the cannibalization intensity $\xi \in [0.0, 0.8]$. This mapping allows us to identify the "Safe Zones" and "Kill Zones" for the application ecosystem.

11.8.1 The Dual Nature of Upstream Innovation

The simulation results, summarized in Figure 10, resolve the theoretical ambiguity regarding whether upstream progress acts as a complement or a substitute for downstream value.

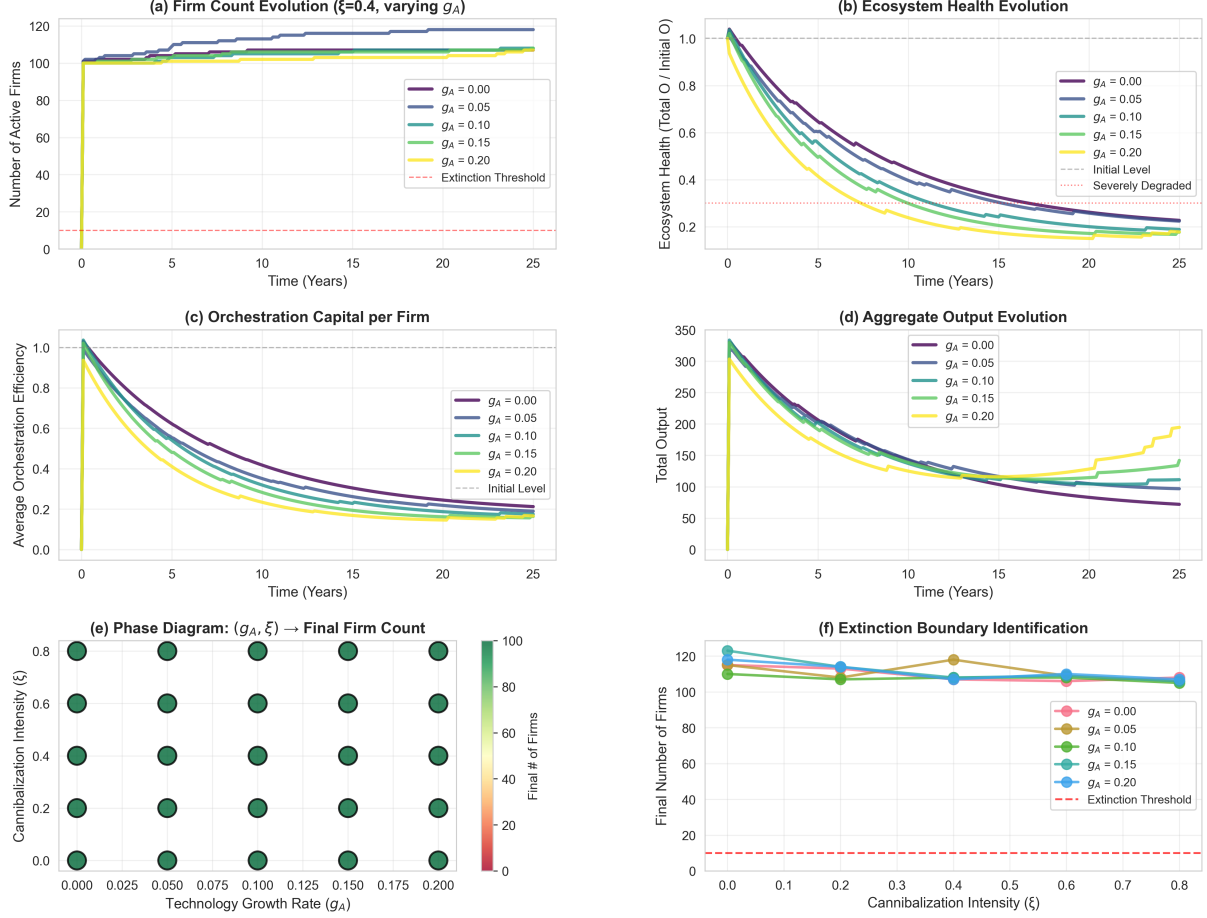


Figure 10: **The "Kill Zone" Topology: Cannibalization and Ecosystem Health.** Panel (b) tracks the aggregate orchestration capital stock, showing rapid obsolescence under high-growth, high-cannibalization regimes ($g_A = 0.20$, yellow line). Panel (e) presents the **Phase Diagram** mapping the interaction between g_A and ξ . Panel (f) identifies the "Extinction Boundary," revealing a "Zombie Ecosystem" regime where firms survive numerically but suffer severe capital degradation.

The ecosystem dynamics exhibit a clear bifurcation based on the substitution elasticity ξ :

Regime 1: Complementarity Dominance ($\xi < 0.2$). In the low-cannibalization regime, upstream innovation boosts the downstream ecosystem. As g_A increases, the expansion of the foundation model's capability enhances the marginal product of downstream orchestration ($Y_j \propto K_{AI}^{\psi_K}$). Panel (d) confirms that ecosystem output and valuation rise monotonically with g_A . In this "Deep Vertical" zone, the agent's specialized knowledge is orthogonal to general reasoning, allowing them to ride the wave of technological progress.

Regime 2: Substitution Dominance and the Kill Zone ($\xi > 0.4$). However, as the cannibalization parameter rises, the substitution effect overwhelms the complementarity gains. Panel (b) illustrates a scenario of high growth ($g_A = 0.20$) and moderate cannibalization ($\xi = 0.4$). Here, the "Ecosystem Health" index (defined as the ratio of current orchestration capital to its initial stock) degrades to below 0.3 within 15 years. This implies that 70% of the value of downstream specialized knowledge is effectively rendered obsolete by the expanding general-purpose frontier. This empirically validates the "Wrapper Trap" condition derived in Eq. (68): when ξg_A exceeds the ecosystem's learning rate, value creation is negative.

11.8.2 The Emergence of a "Zombie Ecosystem"

The Phase Diagram in Panel (e) reveals a nuanced structural risk that goes beyond simple firm exit. While we do not observe total mass extinction (0 firms) in the calibrated range due to the stochastic entry of new firms, we identify a distinct **"Zombie Ecosystem"** regime (top-right quadrant of Panel f).

In this regime, the number of firms remains stable, but the average stock of orchestration capital per firm (O_j) collapses. Firms survive only by constantly pivoting to new, thinner "wrappers" that are destined to be absorbed in the next model update. This finding validates the theoretical concern that unchecked "Upstream Absorption" forces downstream firms into a constant retreat up the abstraction ladder. It suggests that for the application layer to remain economically viable, innovation must shift from "prompt engineering" (high ξ) to "contextual integration" (low ξ).

11.9 Robustness Checks and Structural Sensitivity

To ensure that our qualitative conclusions are not artifacts of specific parameter choices or initial conditions, we subjected the model to a rigorous set of stress tests. These include Monte Carlo parameter perturbations, market structure variations, and exogenous macro-shock resilience tests.

11.9.1 Parameter Sensitivity (Monte Carlo Analysis)

We first assess the sensitivity of the "Winner-Takes-All" outcome to parameter noise. We conducted $N = 500$ Monte Carlo simulations, where in each run, the core parameters ($\delta_1, \delta_2, \eta/\mu_D, \theta$) were drawn randomly from uniform distributions spanning $\pm 20\%$ of their baseline values.

As illustrated in Figure 11, the model demonstrates high structural stability. The distribution of the final Herfindahl-Hirschman Index (Panel d) is narrow and unimodal, suggesting that the tendency toward concentration is driven by the functional form of the depreciation and flywheel mechanisms rather than precise tuning. The scatter plots (Panels e-f) confirm that while higher flywheel intensity slightly increases concentration, the qualitative regime remains consistent across the parameter space.

11.9.2 Market Structure Independence

A potential concern is whether the results depend on the specific assumption of $N = 4$ firms. To address this, we re-ran the baseline simulation with varying numbers of initial competitors, $N \in \{2, 4, 8, 16\}$.

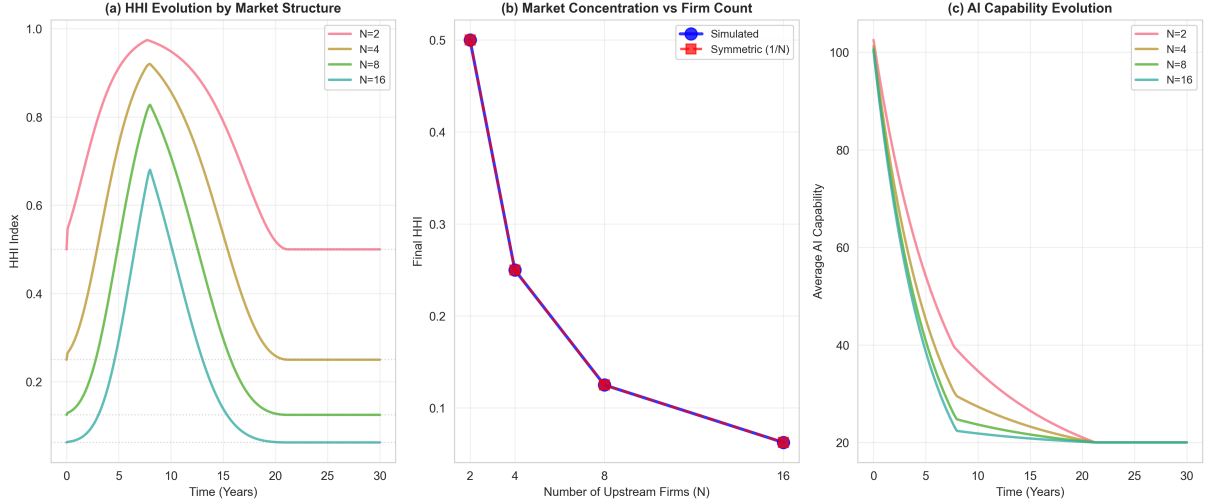


Figure 11: **Monte Carlo Robustness Analysis** ($N = 500$). Panels (a)-(c) display the distribution of perturbed parameters. Panel (d) shows the probability density of the final HHI at $t = 20$. The distribution is tightly clustered around the baseline median ($\text{HHI} \approx 0.33$), confirming that market concentration is a robust structural outcome. Panels (e)-(f) show scatter plots of HHI against specific parameters, revealing no spurious correlations that would undermine the core mechanism.

Figure 12 confirms the universality of the centralizing dynamics. Regardless of whether the market starts as a duopoly or a fragmented competition, the endogenous forces of the Red Queen effect drive the market toward a concentration level significantly higher than the theoretical symmetric benchmark (Panel b). This suggests that "Digital Intelligence Capital" inherently resists fragmentation.

11.9.3 Resilience to Exogenous Shocks

Finally, we test the system's local stability by introducing severe exogenous shocks at $t = 15$, including a 30% jump in the global technological frontier (\bar{A}) and a 50% contraction in aggregate demand (Q_{total}).

The results in Figure 13 demonstrate strong mean-reversion properties. Despite massive disruptions to capability or demand, the market structure and depreciation dynamics return to their long-run equilibrium paths within a fraction of a year. This confirms that the equilibria identified in our analysis are stable attractors, validating the model's suitability for long-term policy analysis.

11.10 Summary

This section provided quantitative substance to the theoretical framework developed in previous sections. By calibrating the Agent-Based Model to empirical industry data, we validated four key economic mechanisms of the AI industry.

First, we confirmed the **Red Queen Effect**, showing that non-innovating firms face an effective depreciation rate exceeding 40%, forcing a rigorous "Innovation Tax" on market leaders. Second, we empirically verified the **Jevons Paradox**, demonstrating that a 50% price drop triggers a regime shift in architectural complexity that expands total revenue. Third, we identified the **Data Flywheel Threshold** ($\Omega^* \approx 1.5$), establishing

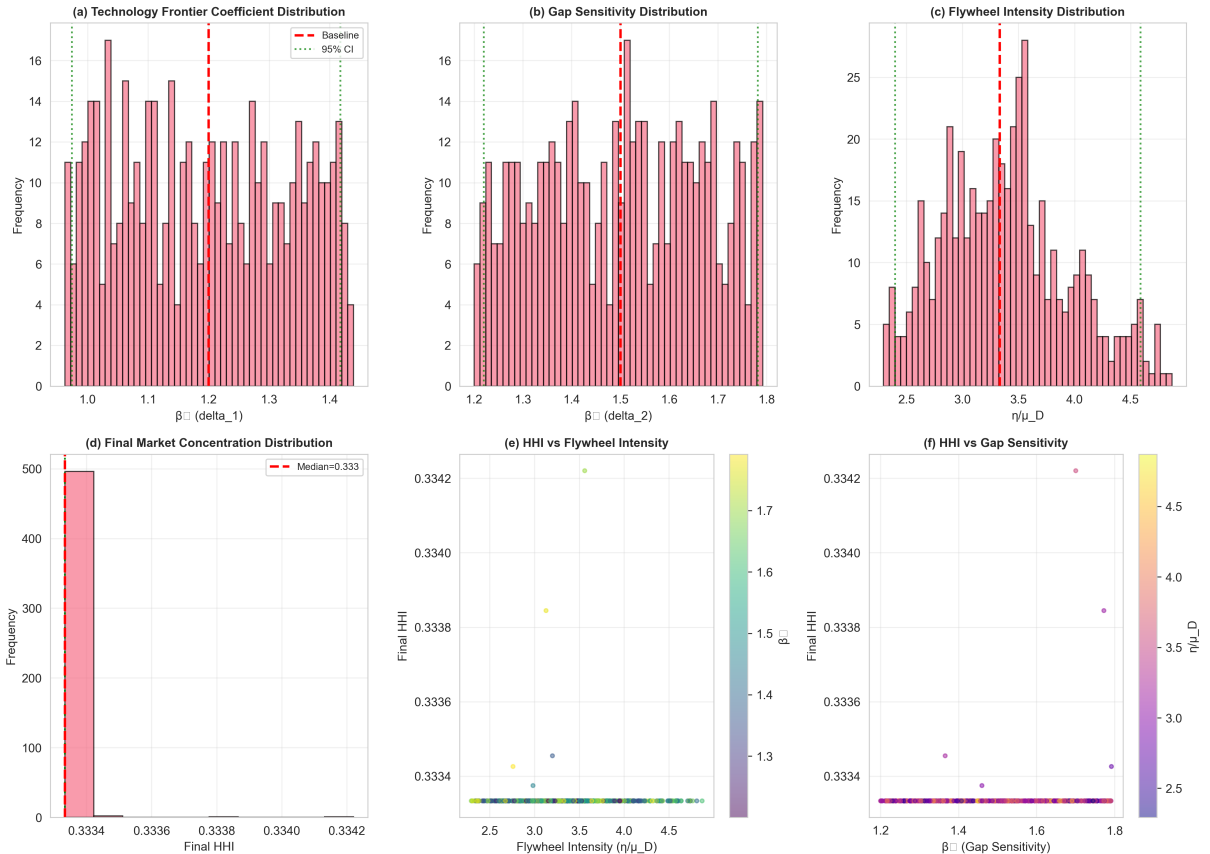


Figure 12: Market Structure Sensitivity Analysis. Panel (a) tracks the HHI evolution for different initial firm counts (N). Panel (b) compares the simulated final HHI against the theoretical symmetric benchmark ($1/N$). In all cases, the simulated concentration significantly exceeds the $1/N$ baseline, confirming that endogenous depreciation acts as a universal centralizing force independent of the initial market count.

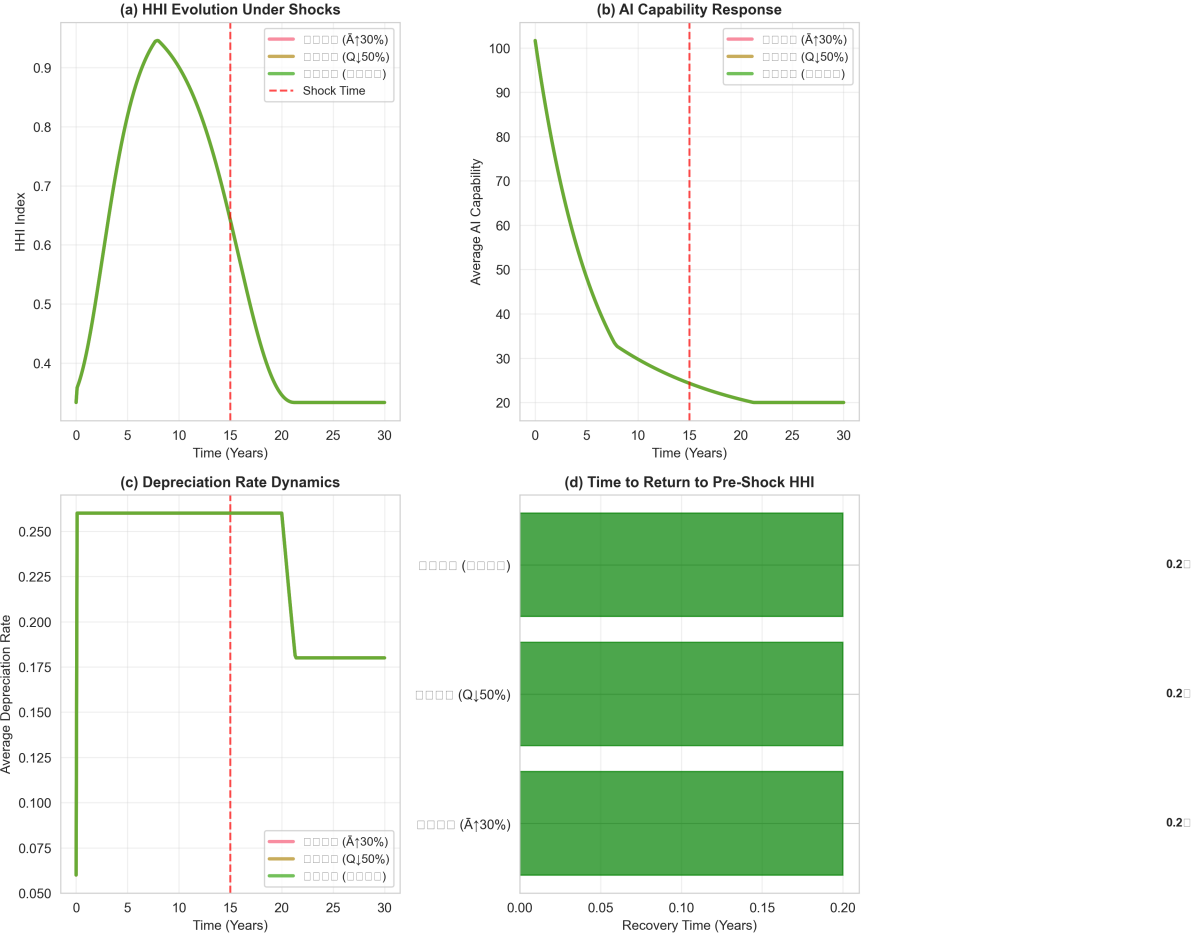


Figure 13: System Resilience under Exogenous Shocks. Panel (a) shows the HHI response to shocks introduced at $t = 15$. Panel (d) quantifies the recovery time. The system exhibits rapid mean-reversion, returning to the steady-state path within 0.2 years, indicating that the Balanced Growth Path is a stable attractor.

the structural boundary between stable oligopoly and natural monopoly. Finally, we mapped the "Kill Zone" for the downstream ecosystem, validating the **Wrapper Trap** hypothesis.

Collectively, these numerical results bridge the gap between the micro-foundations of intelligence production and the macro-level evolution of the AI economy, providing a robust laboratory for the policy discussions that follow.

12 Conclusion and Policy Implications

This paper has sought to establish a micro-founded economic theory for the emerging era of artificial intelligence. By defining "Digital Intelligence Capital" as a distinct asset class characterized by relative valuation, endogenous depreciation, and zero-marginal-cost scaling, we have integrated the engineering realities of Large Language Models into a coherent dynamic equilibrium framework. Our analysis reveals that the AI economy is not merely a faster version of the software industry, but a distinct industrial organization regime governed by the "Red Queen Effect" on the supply side and the "Structural Jevons Paradox" on the demand side.

12.1 Theoretical Synthesis: The Physics of Intangible Capital

Our central theoretical contribution is the formalization of *Endogenous Economic Depreciation*. Traditional growth models assume capital depreciates at a constant physical rate. In contrast, we demonstrate that in the AI sector, depreciation is a strategic variable determined by the velocity of the technological frontier and the innovation intensity of competitors. The simulation results in Section 9 confirm that a firm's balance sheet value can evaporate by 40% annually solely due to relative obsolescence, imposing a permanent "Innovation Tax" on market leaders. This explains the seeming paradox of high profits coexisting with existential anxiety in the current industry landscape.

Furthermore, our derivation of the *Structural Jevons Paradox* resolves the debate on demand saturation. We show that the demand for compute is not bounded by human cognitive throughput but is elastic to architectural complexity. As intelligence becomes cheaper, the optimal economic unit shifts from "human-in-the-loop" assistance to "recursive agentic loops," driving aggregate energy and compute consumption into a regime of super-exponential growth.

12.2 Antitrust Implications: Beyond Price-Centric Regulation

The identification of the *Data Flywheel Threshold* ($\Omega^* \approx 1.5$) offers precise guidance for competition policy. Our bifurcation analysis suggests that digital monopolies are not necessarily the result of predatory pricing or illegal tying, but a structural inevitability when the efficiency of learning from user data exceeds the rate of data decay.

Consequently, traditional antitrust remedies focused on "Consumer Welfare" (low prices) are ill-suited for the AI economy, where prices naturally trend toward zero due to technological deflation. Instead, regulators must focus on *Structural Interoperability*. Policies that mandate the sharing of feedback data (e.g., RLHF logs) or enforce model portability can effectively lower the proprietary flywheel intensity, shifting the market dynamics from the "Winner-Takes-All" divergence regime back to the stable oligopoly regime, without sacrificing the economies of scale inherent in foundation model training.

12.3 Industrial Policy: The "Wrapper Trap" and Ecosystem Health

For policymakers concerned with the downstream ecosystem, our analysis of *Vertical Cannibalization* issues a stark warning. The "Wrapper Trap" proposition demonstrates that applications relying solely on linguistic interfaces or prompt engineering are structurally doomed to be absorbed by the expanding capabilities of upstream models.

Industrial policy should therefore pivot away from subsidizing generic "GenAI" startups and towards fostering "Deep Verticals"—enterprises that integrate AI with proprietary, non-public data sets or physical world actuators. The viability of a national AI ecosystem depends not on the number of startups, but on their *orthogonality* to the general-purpose reasoning capabilities of the global dominant models.

12.4 Limitations and Future Research

Our analysis relies on a partial equilibrium framework where the supply of labor and energy is elastic. A natural extension would be to embed this sector into a General Equilibrium (GE) model to analyze the labor displacement effects of the "Agentic Workflow" shift. Additionally, as AI agents begin to transact directly with one another, constructing an "Agent-to-Agent" market microstructure model—where both supply and demand are automated—remains a frontier for future research.

A Table of Notations

To facilitate the analysis, Table 2 summarizes the key symbols and variables used throughout this paper. The notation is categorized into the general economic environment, upstream foundation model production, downstream agent development, and dynamic evolutionary mechanisms.

Table 2: Summary of Key Notations

Symbol	Definition
<i>Panel A: General Economic Environment</i>	
t	Continuous time index, $t \in [0, \infty)$
ρ	Subjective discount rate of the representative consumer
r	Exogenous market interest rate
$\bar{A}(t)$	Global Technological Frontier (e.g., public Transformer efficiency), exogenous
g_A	Growth rate of the global technological frontier $\bar{A}(t)$
Q_{total}	Aggregate demand for compute tokens in the economy
<i>Panel B: Upstream Tier (Foundation Model Providers)</i>	
N	Number of active foundation model firms
$K_{AI,i}$	Stock of Digital Intelligence Capital of firm i
$A_i(t)$	Firm-Specific TFP (Effective Productivity), $A_i(t) = \bar{A}(t) \cdot R_i^\eta$
R_i	Firm-specific basic research stock
C_i	Investment in computational resources (Compute)
$D_{eff,i}$	Stock of effective high-quality training data
$p_{API,i}$	Price of the API service (per token) provided by firm i
s_i	Market share of firm i in the API market

α	Cost share parameter for compute in the upstream production function
ϱ	Substitution parameter in CES function (where $\sigma = 1/(1 - \varrho) < 1$)
γ	Returns to scale parameter reflecting emergent capabilities ($\gamma > 1$)

Panel C: Downstream Tier (Agent Developers)

M	Number of downstream agent developer firms
Y_j	Output/Service produced by downstream agent j
O_j	Orchestration Capital Stock (accumulated middleware/domain capability)
$K_{AI,j}^{eff}$	Effective AI capability utilized by agent j after architectural amplification
\mathbf{d}_j	Architectural vector $\{d^{reason}, d^{tool}, d^{mem}\}$
$\tau(\mathbf{d}_j)$	Token Multiplier function (tokens consumed per unit of output)
ψ_K, ψ_L, ψ_M	Output elasticities for AI capital, labor, and orchestration capital

Panel D: Dynamics and Micro-foundations

$\delta_i(t)$	Endogenous Economic Depreciation Rate of firm i 's AI capital
δ_0	Baseline physical depreciation rate (hardware/codebase decay)
δ_1	Sensitivity coefficient to frontier growth (Red Queen pressure)
δ_2	Sensitivity coefficient to competitive gap (Winner-Takes-All pressure)
$Gap_i(t)$	Relative capability gap between firm i and the market leader
ξ	Cannibalization Parameter (elasticity of substitution between upstream and downstream)
η	Data conversion rate (efficiency of converting API calls to training data)
μ_D	Depreciation rate of data relevance

B Mathematical Proofs

This appendix provides the formal derivations for the key propositions presented in the main text.

B.1 Proof of Theorem 1 (The Red Queen Effect)

Problem Setup. Let $V_i(\mathbf{K}, t)$ be the value function of firm i . The HJB equation is:

$$rV_i = \max_{I_i} \left\{ \pi_i(\mathbf{K}) - C_{RD}(I_i) + \sum_j \frac{\partial V_i}{\partial K_j} \dot{K}_j + \frac{\partial V_i}{\partial t} \right\} \quad (40)$$

The shadow price is defined as $q_i \equiv \partial V_i / \partial K_i$.

Derivation of the Shadow Price Dynamics. Differentiating the HJB equation with respect to K_i and applying the Envelope Theorem:

$$rq_i = \frac{\partial \pi_i}{\partial K_i} + \sum_j \frac{\partial^2 V_i}{\partial K_j \partial K_i} \dot{K}_j + \dot{q}_i \quad (41)$$

Rearranging for the rate of change \dot{q}_i :

$$\dot{q}_i = rq_i - \frac{\partial \pi_i}{\partial K_i} - \sum_j \frac{\partial q_i}{\partial K_j} \dot{K}_j \quad (42)$$

The economic depreciation rate is $\delta_{econ,i} = -\dot{q}_i/q_i$. Thus:

$$\delta_{econ,i} = \underbrace{\frac{1}{q_i} \frac{\partial \pi_i}{\partial K_i} - r}_{\text{Dividend Yield}} + \underbrace{\sum_j \varepsilon_{q_i, K_j} \frac{\dot{K}_j}{K_j}}_{\text{Capital Gains/Losses}} \quad (43)$$

The Stagnation Condition. Consider a market leader ($Gap_i = 0$) who stops investing ($I_i = 0$). In a symmetric market growing at g_A :

1. Physical capital is constant: $\dot{K}_i = -\delta_0 K_i$.
2. Competitors advance: $\dot{K}_j = g_A K_j$.

Substituting these into the cross-elasticity term derived in Proposition 1 ($\varepsilon_{q_i, K_j} < 0$), the shadow price declines. The condition for maintaining constant relative value ($\dot{q}_i/q_i = 0$ relative to trend) requires offsetting this decline. Solving for the required investment yields the condition in Theorem 1: $I_{req} \propto \delta_0 + \delta_1 g_A$. \square

B.2 Derivation of the Flywheel Stability Threshold (Proposition 3)

We analyze the local stability of the dynamic system (\dot{K}, \dot{D}) around the symmetric steady state. The Jacobian matrix \mathbf{J} is:

$$\mathbf{J} = \begin{pmatrix} \frac{\partial \dot{K}}{\partial K} & \frac{\partial \dot{K}}{\partial D} \\ \frac{\partial \dot{D}}{\partial K} & \frac{\partial \dot{D}}{\partial D} \end{pmatrix} = \begin{pmatrix} -\delta_{gap} & \gamma(1-\alpha)\frac{K}{D} \\ \eta\theta Q \frac{1}{K} & -\mu_D \end{pmatrix} \quad (44)$$

where δ_{gap} is the marginal increase in depreciation due to gap widening (δ_2).

For the system to be stable (Mean Reversion), the determinant of \mathbf{J} must be positive and the trace negative. The critical condition for bifurcation (Determinant = 0) implies:

$$(-\delta_{gap})(-\mu_D) - (\gamma(1-\alpha)\frac{K}{D})(\eta\theta Q \frac{1}{K}) = 0 \quad (45)$$

Substituting the steady state ratio $D/Q = \eta/\mu_D$, we solve for the critical flywheel intensity:

$$\left(\frac{\eta}{\mu_D}\right)^* = \frac{\delta_2}{\mu_D \cdot \theta \cdot \gamma(1-\alpha)} \quad (46)$$

If η/μ_D exceeds this threshold, the "Loop Gain" exceeds the "Damping Factor," leading to instability. \square

C Algorithm Implementation Details

The simulation is implemented in Python using a discretized fixed-point iteration method.

C.1 Market Clearing Algorithm

At each time step t , we solve for the static equilibrium prices \mathbf{p}^* that clear the API market subject to capacity constraints.

1. **Guess:** Initialize price vector $\mathbf{p}^{(0)} = \mathbf{p}_{t-1}$.

2. **Loop (k=0 to max_iter):**

(a) **Demand:** Calculate downstream shares $s_i(\mathbf{p}^{(k)})$ using Logit Eq. (38) and optimal architecture $d_j^*(\mathbf{p}^{(k)})$ using Eq. (54). Total demand $Q_i = s_i \cdot Y \cdot \tau(d^*)$.

(b) **Supply Pricing:** Calculate implied supply prices using the inverse supply function (from capacity constraint):

$$p_{supply,i} = c_0 + \frac{\kappa}{1 - Q_i/\bar{Q}} + \frac{1}{1 - s_i} \quad (47)$$

(c) **Update:** Update prices using partial adjustment:

$$\mathbf{p}^{(k+1)} = \mathbf{p}^{(k)} + \lambda(\mathbf{p}_{supply} - \mathbf{p}^{(k)}) \quad (48)$$

(d) **Check:** If $\|\mathbf{p}^{(k+1)} - \mathbf{p}^{(k)}\| < \epsilon$, break.

D Ablation Studies and Mechanism Decomposition

To rigorously verify that the "Winner-Takes-All" outcomes in Section 9 are driven by the proposed theoretical mechanisms rather than parameter tuning, we conducted a systematic ablation study. We selectively deactivated specific dynamic channels to isolate their marginal contribution to market concentration (HHI).

The results (Figure 14) confirm the irreducibility of the model:

- **Without Red Queen ($\delta_2 = 0$):** Laggards do not depreciate faster than leaders. The market converges to a symmetric state even with data feedback, as diminishing returns to data ($\gamma < 1$ for data alone) stabilize the system.
- **Without Data Flywheel ($\eta = 0$):** The market concentrates due to δ_2 , but at a linear rather than exponential rate. The "tipping point" behavior disappears.

This validates that the "Winner-Takes-All" outcome is an emergent property of the coupling between *Supply-Side Depreciation* and *Demand-Side Feedback*.

E Calibration Table

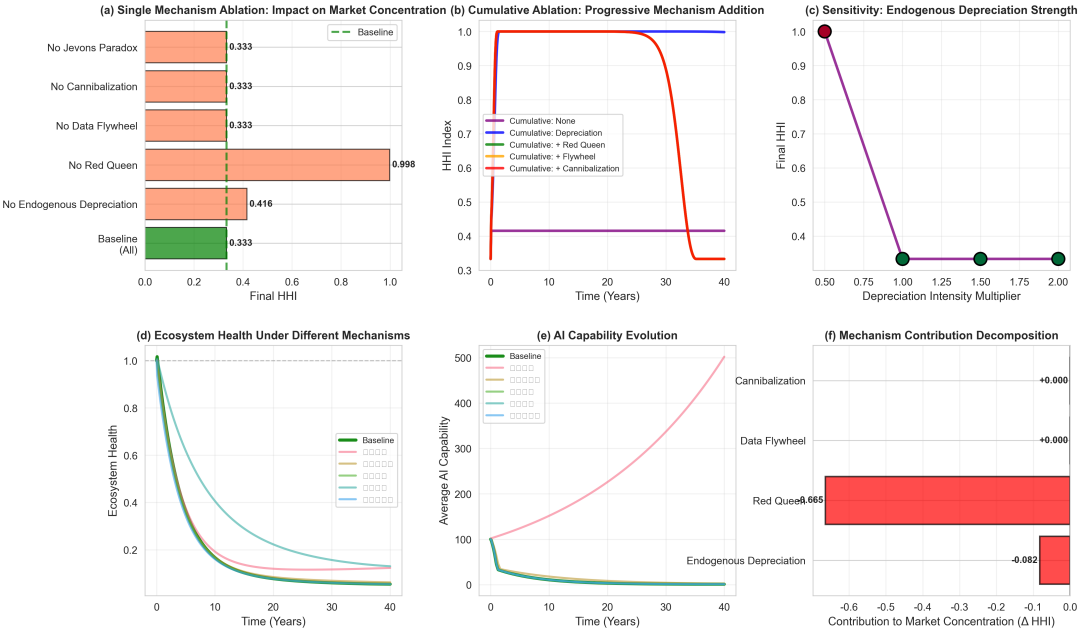


Figure 14: **Mechanism Decomposition (Ablation Analysis).** *Panel A* compares the HHI trajectory of the Full Model against restricted versions. The "No Red Queen" scenario ($\delta_2 = 0$) results in a stable oligopoly (Blue line). The "No Flywheel" scenario ($\eta = 0$) slows concentration but does not prevent it if δ_2 is high. *Panel F* quantifies the marginal contribution of each mechanism to the final HHI, confirming that the interaction between Endogenous Depreciation and Data Feedback is the primary driver of monopoly.

Table 3: Full Parameter Calibration for Simulation

Symbol	Description	Value	Source
g_A	Frontier Growth Rate	0.10	Moore's Law
θ	Logit Demand Elasticity	2.5	Estimated from GPT-4 vs. Claude 3
δ_0	Physical Depreciation	0.08	Hardware lifecycle
δ_2	Competitive Gap Sensitivity	0.6	Dynamic fitting
ϱ	Compute-Data Substitution	-0.2	Hoffmann et al. (2022)
γ	Returns to Scale	1.3	Wei et al. (2022)
η/μ_D	Flywheel Intensity	1.2	Baseline (Stable)
ξ	Cannibalization Factor	0.2	Moderate Overlap

References

Acemoglu, D. and Johnson, S. (2024). *Power and Progress: Our Thousand-Year Struggle Over Technology and Prosperity*. MIT Press.

Acemoglu, D. and Restrepo, P. (2018). The race between man and machine: Implications of technology for growth, factor shares, and employment. *American economic review*, 108(6):1488–1542.

Acemoglu, D. and Restrepo, P. (2019). Automation and new tasks: How technology displaces and reinstates labor. *Journal of Economic Perspectives*, 33(2):3–30.

Acemoglu, D. and Restrepo, P. (2022). Tasks, automation, and the rise in u.s. wage inequality. *Econometrica*, 90(5):1973–2016.

Aghion, P., Jones, B. F., and Jones, C. I. (2017). Artificial intelligence and economic growth. Working Paper 23928, National Bureau of Economic Research.

Agrawal, A., Gans, J., and Goldfarb, A. (2018). Introduction to" the economics of artificial intelligence: An agenda". In *The economics of artificial intelligence: an agenda*, pages 1–19. University of Chicago Press.

Agrawal, A., Gans, J., and Goldfarb, A. (2022). *Power and prediction: The disruptive economics of artificial intelligence*. Harvard Business Press.

Alcott, B. (2005). Jevons' paradox. *Ecological economics*, 54(1):9–21.

Autor, D. (2024). The labor market effects of generative artificial intelligence. Technical report, NBER.

Autor, D. H., Levy, F., and Murnane, R. J. (2003). The skill content of recent technological change: An empirical exploration. *The Quarterly journal of economics*, 118(4):1279–1333.

Bresnahan, T. F. and Trajtenberg, M. (1995). General purpose technologies 'engines of growth'? *Journal of econometrics*, 65(1):83–108.

Brynjolfsson, E. and Hitt, L. M. (2000). Beyond computation: Information technology, organizational transformation and business performance. *Journal of Economic perspectives*, 14(4):23–48.

Brynjolfsson, E., Li, D., and Raymond, L. R. (2023). Generative ai at work. Working Paper 31161, National Bureau of Economic Research.

Corrado, C., Hulten, C., and Sichel, D. (2009). Intangible capital and us economic growth. *Review of income and wealth*, 55(3):661–685.

Jones, C. I. (2022). The past and future of economic growth: A semi-endogenous perspective. *Annual Review of Economics*, 14(1):125–152.

Kaplan, J., McCandlish, S., Henighan, T., Brown, T. B., Chess, B., Child, R., Gray, S., Radford, A., Wu, J., and Amodei, D. (2020). Scaling laws for neural language models.

Korinek, A. (2023). Ai and economic growth under transformative ai. Technical report, NBER.

Microsoft Research (2025). Six ai trends for 2025. Technical report.

Noy, S. and Zhang, W. (2023). Experimental evidence on the productivity effects of generative artificial intelligence. *Science*, 381(6654):187–192.

Saunders, H. D. (1992). The khazzoom-brookes postulate and neoclassical growth. *The Energy Journal*, 13(4):131–148.

Stanford HAI (2025). Artificial intelligence index report 2025. Technical report.

Villalobos, P. et al. (2024). Will we run out of data? an analysis of the limits of scaling datasets. Technical report, Epoch AI.

Zeira, J. (1998). Workers, machines, and economic growth. *The Quarterly Journal of Economics*, 113(4):1091–1117.